INVESTIGATIONS OF SPONTANEOUS CONDENSATION PHENOMENA

Thesis by

Richard M. Head

In Partial Fulfillment of the Requirements

For the Degree of

Doctor of Philosophy

California Institute of Technology

Pasadena, California

1949

ACKNOWLEDGMENTS

The author is deeply grateful to Dr. H. W. Liepmann, who suggested this research topic, and whose guidance and constructive criticism throughout the course of the investigation have been a constant source of inspiration.

The author wishes to express his appreciation to Dr. C. B. Millikan, Mr. A. E. Puckett, and Dr. F. E. Marble, in particular, for their valuable criticisms and suggestions throughout the course of the work.

Messrs. Ashkenas, Roshko, Dhawan, and Barnett were extremely helpful in the performance of various aspects of the experimental program and the author is sincerely appreciative of their invaluable assistance.

SUMMARY

The results of a systematic wind tunnel investigation into the attainment and ultimate collapse of the supersaturated state of water vapor are presented. These results, together with those of other recent investigations, are collected and compared with the theory. It is found that the deviations from the quasi-stationary conditions upon which the theory is based are very pronounced in the supersonic wind tunnel. A much higher degree of supersaturation can, therefore, be attained before condensation occurs than is predicted theoretically.

Measurements at low temperatures indicate that if the water vapor reaches a temperature of about 153° K. without the occurrence of condensation, the vapor will not condense upon further expansion, regardless of how highly supersaturated it becomes. This observation is in agreement with some recent Wilson Cloud Chamber investigations.

The shock relations for flow involving condensation are discussed. It is shown that two types of discontinuities can occur; the condensation shock and the shock with condensation (or vaporization). The latter solution has been disregarded in the past, but it is shown that the shock with vaporization is of importance and can result in appreciable errors in Mach number determination when droplets are present in the flow.

Various techniques of measurement of the condensation processes in supersonic flow are considered.

CONTENTS

PART I

INTRODUCTION AND SURVEY OF THE LITERATURE

The phenomenon of spontaneous condensation, or the transition of a substance from the vapor phase into the liquid phase in the absence of a plane surface of the liquid phase, has been the subject of numerous experimental investigations for the past sixty years. It was not until the advent of the supersonic wind tunnel, however, that this phenomenon entered the field of aeronautics and even then it was not recognized as such until about 1940. The condensation in this case manifests itself by a sudden increase in pressure, with an attendant formation of a fog of liquid droplets or ice particles, at some point in the supersonic section of the nozzle. This pressure increase troubled many early investigators, but the fog is usually not readily visible except under certain lighting conditions and hence the true explanation was overlooked for several years.

In a supersonic nozzle, air containing water vapor undergoes an adiabatic expansion which, accordingly, results in a continuous decrease in temperature and pressure. The saturation vapor pressure, which depends upon the temperature only, decreases much more rapidly than does the partial pressure of the water vapor and hence saturation is approached and even exceeded. If a calculation is made of the relative humidity of the air at the point where the condensation occurs, it is found that the air is highly supersaturated. The first person to call attention to the fact that a highly supersaturated vapor can exist

under certain conditions was R. v. Helmholtz.[1] He showed, in 1887, that a saturated steam jet expanding from an orifice into the atmosphere remained perfectly clear for some distance and then suddenly became cloudy.

Helmholtz also demonstrated the effect of ions on the initiation of condensation by observing the increased cloudiness that resulted when an electrical discharge coursed the jet. Ions and, particularly, hygroscopic nuclei are of prime importance in initiating condensation in the atmosphere. This is due to the fact that such nuclei range in size from 10^{-3} to 10^{-6} cm. in radius and, as will be shown in Part II, the effect of curvature on the equilibrium of water deposited on such nuclei is relatively small. Furthermore, if the hygroscopic nuclei are active solutes, as is generally the case in the atmosphere, the surface tension will be greatly lowered. These two effects can give rise to the formation of droplets which are in equilibrium with unsaturated air. As a result of these factors, together with the fact that the changes of state of the air proceed at a relatively slow rate, large supersaturations have never been observed in the atmosphere.

Wilson Cloud Chamber Investigations

The Wilson Cloud Chamber, which was developed by C. T. R. Wilson [2] in 1897, utilizes this fact that ions facilitate the initiation of condensation.

The air in a Wilson Cloud Chamber is contained in a closed vessel and is cooled adiabatically by suddenly increasing the volume by means of a piston. In normal practice, the air is saturated at the initial

temperature and volume and various degrees of supersaturation are obtained by varying the expansion ratio, i.e., by varying the final position of the piston. Different degrees of supersaturation can be attained at the same final temperature by increasing the initial temperature as the expansion ratio is increased. The supersaturation is gradually increased in this manner until a cloud forms, the value at which this occurs being denoted as the "threshold supersaturation ratio" corresponding to the particular final temperature.

Inasmuch as the air is essentially at rest and is cooled much less rapidly than it would be in a wind tunnel, the results are not directly applicable to the problem of condensation in rapidly expanding gases. However, since the existing theories of spontaneous condensation are based on the assumption of a quasi-stationary state, which is closely approximated in the Wilson Cloud Chamber, and since the effect of foreign nuclei is clearly demonstrated in these experiments, it will be of value to review briefly the pertinent results.

Powell [3] observed that, for the same final temperature, higher and higher supersaturations were required as the outdoor air used in the experiment was progressively filtered. Filtered air containing ions necessitated greater expansions than unfiltered air, while ion-free filtered air required still greater expansions. Powell's results for dust-free, ion-free air of the supersaturation required for condensation as a function of the final temperature are plotted in Fig. 1.

Sander and Damköhler [4] performed a similar set of experiments, the results of which are plotted in Fig. 1, also. The quantitative agreement between these results and those of Powell is, for some unknown reason, not very good.

Formation of Liquid Droplets or Ice Crystals

Several recent Cloud Chamber investigations by Cwilong [5] and Fournier d'Albe [6] have been concerned with the determination of the final temperature at which ice crystals form instead of water droplets. Cwilong observed that, with dust-free air, below a temperature of -42° C. the cloud is composed of ice crystals and water droplets, while above this temperature ice crystals are absent. With unfiltered outdoor air this transition temperature increased to -32° C., although Fournier d'Albe observed that, even though ice particles were formed at this temperature, water droplets still predominated.

This mixture of ice particles and water droplets, for dust-free air, was observed down to -65° C. to -70° C., below which ice particles only were present. Sander and Damköhler observed liquid droplets down to -62° C. On the basis of these observations and in view of the lack of evidence one way or the other from wind tunnel measurements, it will be assumed in the analysis of the spontaneous condensation phenomenon that the condensation is in the form of liquid droplets down to 210° K. (-63° C.).

The effect of ions on the condensation of dust-free air at temperatures below -55° C. has apparently not yet been established. The observation that the presence of ions does not affect the supersaturation at

which condensation occurs when the temperature is below -60° C. has been confirmed by several investigators. However, the observation of Cwilong, that the presence of ions at these temperatures results in the formation of a greater number of ice particles than in ion-free air, is in contradiction to the observations of Fournier d'Albe, who noted no effect upon irradiating the chamber with gamma rays. Thus, this particular question is in need of further investigation.

One observation of Cwilong's, that was mentioned briefly by him, has startling implications when considered from the viewpoint of spontaneous condensation in high speed wind tunnels. This observation was that when the temperature at the end of the expansion falls below -120° C. no products of condensation, neither liquid droplets nor ice particles, are observed. This finding is of such theoretical and experimental importance as to warrant a separate treatment in Part VI.

Steam Nozzle Investigations

The existence of supersaturation and the spontaneous collapse of the supersaturated state in connection with the expansion of a vapor in nozzles was recognized first in 1903, as a result of the comprehensive tests of Stodola (7) utilizing superheated steam. Since that time a number of investigations have been made in an effort to determine the supersaturation ratios at which spontaneous condensation takes place. The location of the collapse of the supersaturated state in these cases was determined either by pressure measurements or by the light scattering technique initiated in this field by Stodola. In view of this wealth of information it is surprising indeed that the phenomenon of spontaneous

condensation was unrecognized in supersonic wind tunnels for a number of years.

The use of superheated steam, and hence high stagnation temperatures, results in the condensation occurring at local temperatures of the order of 300° K. and higher. Such temperatures are much higher than those normally found in supersonic tunnels. The results of these investigations are of more than academic interest, however, in that they significantly extend the temperature range over that obtainable from supersonic wind tunnel tests alone.

Of the most recent of the superheated steam experiments, those of Yellott [8], Yellott and Holland [9], Rettaliata [10], and Binnie and Woods [11], the measurements of Binnie and Woods appear to be the most reliable and hence their results are shown in Fig. 1 in the form of threshold supersaturation ratio vs. local temperature.

Supersonic Wind Tunnel Investigations

The first investigations of spontaneous condensation in supersonic wind tunnels were performed by Hermann and Wieselsberger [12] during the years 1934 to 1936, although their results were not published until 1942. Hermann presents qualitative findings of the effect of relative humidity and water vapor content of the air on the location and strength of the so-called "condensation shocks" or "X-shocks" which he observed by means of a Schlieren system. He also extended the one-dimensional shock relations to the case of normal shocks involving condensation, but inasmuch as this analysis was brief and incomplete, it will be considered in more detail in Appendix I.

The only systematic investigation of the phenomena of spontaneous condensation in supersonic wind tunnels from the theoretical point of view has been that by Oswatitsch (13) and (14).

Through considerations of the equations for the conservation of mass, momentum and energy, Oswatitsch, in his first paper (13), develops a system of differential equations describing the compressible flow of humid air containing droplets of water or ice through a nozzle. These equations, together with the equation for the rate of formation and growth of the droplets, enable him to perform a step-by-step calculation of the pressure distribution in a nozzle with condensation. These theoretical results are in excellent agreement with the pressure distribution measurements of Yellott* and Binnie and Woods* using superheated steam. The equation for the rate of formation of droplets utilized by Oswatitsch is due to Becker and Döring and will be discussed in Part II. By dealing with a simplified picture of a droplet of water in pure water vapor and considering the molecular processes at the surface as providing for the necessary mass transport onto the droplet and the removal of the heat of condensation from the droplet, Oswatitsch arrives at an equation for the droplet growth. In view of the excellent agreement between the theoretical pressure distributions and the experimental ones using superheated steam, it may be concluded that this equation for the growth of a droplet in its vapor is an accurate description of the process. However, as pointed out by Oswatitsch, this equation is no longer valid in the case of a droplet situated in supersaturated humid

---

* loc. cit.

air, where diffusion is primarily responsible for providing for the necessary mass transport. Hence, no comparison can be made between the theoretical calculations and the experimental results using humid air in view of the lack of knowledge as to the equation for the droplet growth. Furthermore, in the experiments with superheated steam, the local temperatures at which spontaneous condensation takes place are still of the order of room temperatures or higher, where the values of the surface tension of water are well known; whereas in most supersonic wind tunnels the local temperatures are in the range where no data exists on either the surface tension of water or the surface energy of ice, which, as will become evident, are so important for the determination of the droplet formation frequency.

Oswatitsch also presents the results of his experimental investigation in a supersonic nozzle, using humid air of three different relative humidities at atmospheric stagnation conditions. These results were obtained in the form of pressure distribution measurements along the nozzle, from which the supersaturation ratio at the location of collapse of the supersaturated state has been calculated and plotted in Fig. 1 as a function of the local temperature at that location.

Oswatitsch, in his second paper (14), deals with the theoretical aspects of condensation in humid air flowing through a nozzle. He was able to show that the condensation on foreign nuclei in the air and the subsequent growth of the droplets was too small to cause any measurable deviation from the dry-adiabatic expansion. This conclusion is the result of the relatively small number of foreign particles in normal

laboratory air (of the order of $10^6/cm^3$, and the short time available for the growth of drops. The negligible effect of condensation on foreign nuclei leads to high degrees of supersaturation, where spontaneous condensation of the water vapor may take place. On the basis of the Becker-Döring equation, a law of droplet growth derived on the assumption of exceedingly small droplets, and certain order-of-magnitude calculations, Oswatitsch arrives at an equation for determining the location of the start of spontaneous condensation. The temperature at which spontaneous condensation takes place is found to depend upon the saturation temperature for adiabatic expansion, which takes the stagnation pressure and specific humidity of the humid air into account, and the temperature gradient, which takes account of the scale effects. This approximate equation is presumably valid provided the temperature gradient is not less than 10° C./cm., since below this value the droplet growth law used in the determination of the equation loses its validity. One constant is left undetermined in the equation, and its value is calculated by Oswatitsch on the basis of the three experimental points obtained from his aforementioned investigation. This final equation is shown in Fig. 1 in the form of the supersaturation ratio at the start of spontaneous condensation vs. the local temperature, for three different values of the temperature gradient.

Contributions of Charyk

Charyk [15] presented the Becker-Döring theory, which will be discussed briefly in Part II, and calculated, therefrom, the supersaturation ratio at which the collapse of the supersaturated state takes place as a

function of the local temperature (Fig. 1) under the assumption that the nuclei formation frequency, J (the number of droplets formed per cubic centimeter per second), is equal to 1,000*.

From one-dimensional considerations, Charyk also develops the equations for the change in flow parameters across a normal condensation shock (see Appendix I) and extends the results to the oblique condensation shock. In addition, a discussion is given of the possibility of continuous condensation downstream of a condensation shock. This condition may arise when the water vapor content of the air is so high that, if an amount sufficient to bring the air down to saturation were to be condensed out at the shock, an amount of heat would be released that is higher than the maximum amount the stream can absorb**. Hence, in this case, the air would be supersaturated downstream of the condensation shock and continuous condensation would occur until a saturated state was reached.

Experimental Investigations of the NACA

In a very recent experimental investigation by the NACA (16), a systematic study of the degree of supersaturation just prior to the collapse of the supersaturated state was made in the Mach number range from 1.4 to 2.0. Two wind tunnels were used in this investigation and each was equipped with wall orifices for the static pressure measurements.

---

* Charyk points out that the difference in the locus of condensation for $J = 1$ and $J = 1{,}000$ is negligible. However, it is found, as will be shown later, that values for J as high as 10^{16} have to be considered, in which case the locus is markedly different.

** See Equation I.16, Appendix I.

During each run, the initial water vapor content was held constant while the stagnation temperature was increased step-by-step from room temperature up to about 200° F. Hence, the location of the start of condensation was gradually moved downstream past successive static pressure holes and thus the conditions prior to the collapse could be determined at various Mach numbers. Several different values of the initial water vapor content were used, from which the effect of this quantity on the condensation phenomena could be determined.

The results of these investigations have been calculated in the form of the threshold supersaturation ratio vs. the local temperature and are shown in Fig. 1.

These results have been extended by the authors, on a theoretical basis, to higher Mach numbers. However, such an extrapolation is questionable in view of the low temperature effects discussed in Part VI.

Miscellaneous Experimental Investigations

Within the past few years, there have been a number of other experimental investigations into the phenomena of spontaneous condensation in supersonic wind tunnels. However, most of these have not been systematic enough to supply the data needed to determine the threshold supersaturation ratio and thence add to our knowledge on the effects of scale.

Thus, the only additional published data, known to the author, that is of value in this investigation, is that of Redington [17], who made pressure distribution measurements in an induction-type

supersonic wind tunnel at various values of initial water vapor content and relative humidity. These results have been calculated in the form of threshold supersaturation ratio vs. temperature, also, and are presented in Fig. 1.

Purpose of the Present Investigation

At the inception of the present research program (1946), the only existing experimental data on the spontaneous condensation phenomena were those obtained from the superheated steam experiments, the Wilson Cloud Chamber and the brief investigation of Oswatitsch. The Wilson Cloud Chamber data, as has been pointed out, are primarily of value in understanding the phenomena under quasi-stationary conditions. The dynamic effect, i.e., the deviation from the quasi-stationary state, discussed in Parts II-A and V, together with the high temperature at which the condensation takes place, in the flow of superheated steam is such that the data obtained therefrom are not directly applicable to the problem of the spontaneous condensation in a mixture of water vapor and air flowing in a supersonic wind tunnel.

Hence, the need existed for a systematic investigation of the problem from the viewpoint of the supersonic wind tunnel. Such an attack was necessary from the practical point of view in order that a criterion for condensation-free flow in supersonic wind tunnels could be developed to provide a basis for the design of wind-tunnel drying equipment. Of much more importance, from the theoretical viewpoint, was the need for an understanding of the mechanism of the spontaneous collapse of the supersaturated system. A mechanism

had been propounded from purely theoretical considerations and it was desirable to determine a) whether the theory adequately explains the process under the assumptions involved or whether the process takes place in a region where the theory is invalid, b) the dynamic and scale effects, assuming the theory is correct for a quasi-stationary state, c) information as to the value of the surface tension of water at low temperatures and for very small droplets, where no data exist at the present time, by working backward from the experimental data under the assumption that the theory is valid, d) the effects of low temperature and e) the change in flow parameters downstream of the region of spontaneous condensation.

From the results of the present investigation a number of these aims have been accomplished; however, much additional work is needed before the mechanism of spontaneous condensation can be said to be completely understood.

PART II

THERMODYNAMIC FUNDAMENTALS

The Isentropic Expansion of a Vapor

Any vapor whose latent heat is large will approach saturation when it is cooled by means of an isentropic expansion and, if the expansion is carried far enough, will reach a supersaturated state. Saturation is defined here in the standard manner, namely, a vapor is saturated when it is in equilibrium with a plane surface of its liquid or solid phase at the same temperature, as many molecules passing in unit time from the liquid or solid to the vapor phase as from the vapor to the liquid or solid phase. The partial pressure of the vapor is independent of the presence of other vapors or gases, being a function of temperature only. A vapor and a gas are distinguished here according to their true definitions; i.e., the substance is called a gas if its temperature is above the critical temperature, while if its temperature is below this value it is called a vapor.

The requirement of an isentropic expansion rather than compression of a vapor of large latent heat in order to produce saturation, may be shown in the following manner (in all following analyses, the vapor is assumed to follow the perfect gas law, an assumption that is in general well justified in the present application):

Consider a vapor undergoing an isentropic process

$$P_v = \text{constant} \cdot T^{\frac{\Gamma}{\Gamma-1}} \qquad (2.1)$$

or, differentiating logarithmically,

$$\frac{dp_v}{p_v} = \frac{\Gamma}{\Gamma-1}\frac{dT}{T} \tag{2.2}$$

whence,

$$\frac{dp_v}{dT} = \frac{\Gamma}{\Gamma-1}\frac{p_v}{T} = c_{p_v}\cdot\frac{p_v}{\frac{R}{m_v}T} \tag{2.3}$$

$c_p \sim \frac{\text{energy}}{\text{mass deg}}$

where, Γ = ratio of the specific heats of the vapor

R = universal gas constant

m_v = molecular weight of the vapor.

These equations are, in general valid only when the vapor is in a pure state. If, for example, a mixture of water vapor and dry air were to undergo an isentropic change of state, it can be shown that the entropy of both the water vapor and the dry air will change during the process.

The entropy of the mixture of dry air and water vapor is

$$Wds = W_a ds_a + W_v ds_v = 0$$

or,

$$ds_a + x ds_v = 0 \tag{2.4}$$

where the subscripts "a" and "v" refer to dry air and water vapor, respectively, and $x = \frac{W_v}{W_a}$ is the ratio by weight of the water vapor to the dry air in a given volume of humid air. x is called the mixing ratio and is related to the specific humidity, $q = \frac{W_v}{W_a + W_v}$, by the expression

$$q = \frac{x}{1 + x},$$

Utilizing the Second Law of Thermodynamics, equation (2.4) becomes

$$c_{p_a} \frac{dT}{T} - \frac{R}{m_a} \frac{dp_a}{p_a} + x\left(c_{p_v} \frac{dT}{T} - \frac{R}{m_v} \frac{dp_v}{p_v} \right) = 0 \qquad (2.5)$$

Since the mixing ratio remains constant for a given mass of humid air as long as there is no evaporation, condensation or mixing with air masses of different mixing ratio, it follows that

$$x = \frac{w_v}{w_a} = \frac{\rho_v}{\rho_a} = \varepsilon \frac{p_v}{p_a} \qquad (2.6)$$

where

$$\varepsilon = \frac{m_v}{m_a}$$

or, differentiating logarithmically,

$$\frac{dp_v}{p_v} = \frac{dp_a}{p_a} = \frac{dp}{p} \qquad (2.7)$$

Combining equations (2.5) and (2.7):

$$\frac{dT}{T} = \frac{R\left(\frac{1}{m_a} + \frac{x}{m_v}\right)}{c_{p_a} + x c_{p_v}} \cdot \frac{dp}{p} \qquad (2.8)$$

Thus, the change in entropy of the dry air or water vapor, as the mixture undergoes an isentropic process, is obtained from equations (2.8) and (2.5):

$$ds_a = \left[c_{p_a} \cdot \frac{R_1\left(\frac{1}{m_a} + \frac{x}{m_v}\right)}{c_{p_a} + x\, c_{p_v}} - \frac{R}{m_a} \right] \frac{dp_a}{p_a}$$

$$= \frac{R}{m_a} \cdot \frac{dp_a}{p_a} \left[\frac{1 + \frac{x}{\varepsilon}}{1 + x \cdot \frac{c_{p_v}}{c_{p_a}}} - 1 \right] \qquad (2.9)$$

and

$$ds_v = \frac{R}{m_v} \frac{dp_v}{p_v} \left[\frac{\varepsilon + x}{\frac{c_{p_a}}{c_{p_v}} + x} - 1 \right] = -\frac{ds_a}{x} \qquad (2.10)$$

Hence, the water vapor and the dry air would undergo isentropic changes of state only if $\varepsilon = c_{p_a}/c_{p_v}$, i.e., if $m_v c_{p_v} = m_a c_{p_a}$. Assuming a value for x of 0.02, which corresponds approximately to that of air saturated with water vapor at standard pressure and a temperature of 300° K., the factor on the right hand side of equation (2.10) becomes $\left[\frac{0.642}{0.535} - 1 \right] = 0.20$ and hence cannot ordinarily be considered negligible*.

The equation for the variation of the partial pressure of water vapor with temperature, corresponding to equation (2.3) for a pure vapor, is obtained from equation (2.8) as

$$\frac{dp_v}{dT} = c_{p_v} \cdot \frac{p_v}{\frac{R}{m_v} T} \left(\frac{\frac{c_{p_a}}{c_{p_v}} + x}{\varepsilon + x} \right) \qquad (2.11)$$

---

* Reference should be made to Appendix III for the possible errors involved in neglecting the presence of water vapor in the air in the determination of Mach number, T/To, etc. in supersonic nozzles.

The variation of the saturation vapor pressure with temperature is related to the latent heat of vaporization by the Clausius-Clapeyron equation

$$\frac{dp_\infty}{dT} = \frac{L}{T} \cdot \frac{1}{v_v - v_\ell} \tag{2.12}$$

where P_∞ is the saturation vapor pressure corresponding to a particular temperature, L is the latent heat of vaporization and v_v and v_ℓ are the specific volumes of the vapor phase and liquid phase, respectively. Neglecting the specific volume of the liquid phase relative to the vapor phase, equation (2.12) becomes

$$\frac{dp_\infty}{dT} = \frac{L}{T v_v} = \frac{L}{T} \cdot \frac{p_v}{\frac{R}{m_v} \cdot T} \tag{2.13}$$

By comparing equation (2.13) with (2.3) or (2.11), it is seen that if $L/T > Cp_v$ then the saturation vapor pressure increases with increasing temperature more rapidly than does the vapor pressure. Hence, with decreasing temperature, as in an expansion, the ratio P_v/P_∞, called the relative humidity or supersaturation ratio, continually increases until saturation and supersaturation are obtained. The ratios of equation (2.13) to (2.3) and of (2.13) to (2.11) as a function of temperature are plotted in Fig. 2 for pure water vapor and for water vapor in air.

The two main components of air, nitrogen and oxygen, become vapors below their critical temperatures of 126° K. and 154° K., respectively. Hence, it is to be expected that, as an expansion proceeds to temperatures below these values, saturation and supersaturation with respect to either,

or both, of these components will be reached.

The same development as was used in equations (2.4) through (2.11) for a mixture of water vapor and dry air is valid for a mixture of nitrogen and oxygen. However, in this case it is apparent that both the nitrogen and oxygen undergo an isentropic change of state since, referring to equation (2.10), $m_{N_2} c_{p_{N_2}} = m_{o_2} c_{p_{o_2}} = 3.47$ at $0^\circ C$. Hence, both the nitrogen and oxygen expand independently of the other and equation (2.3) can be used directly.

The rates of approach to saturation, $\frac{dp_\infty}{dT} \Big/ \frac{dp_v}{dT}$, for both nitrogen and oxygen are plotted in Fig. 2, also. Included, too, as a matter of interest, are the values for pure carbon dioxide and for carbon dioxide in air.

It is interesting to note, from Fig. 2, that the rate of approach to saturation of the water vapor in air is, for a given temperature, approximately 20% greater than that of pure water vapor. Hence, for the same rate of expansion, the water vapor in air becomes supersaturated more quickly than does the pure water vapor.

The fact that all the curves start from zero shows that, for the vapors considered herein, an isentropic expansion produces a decrease in the supersaturation until the temperature corresponding to a value of unity for $\frac{dp_\infty}{dT} \Big/ \frac{dp_v}{dT}$ is reached. Continual expansion then causes the supersaturation to start increasing. Similarly, for any vapor whose latent heat is small, i.e., $L < Cp_v T$, an isentropic compression is required in order for saturation to be approached.

In considering the possibility of oxygen and/or nitrogen condensation in the light of present-day experience with water vapor condensation, one important factor that is often overlooked is that at corresponding temperatures the latent heat of water is of the order of ten times that of either nitrogen or oxygen and hence the pressure increase*, when condensation of the nitrogen or oxygen does occur, will be much less significant than in the case of water vapor condensation.

B. The Change in the Supersaturation of a Vapor on Passing Through a Shock Wave.

In the preceding section it was seen that the isentropic expansion of an unsaturated vapor results in saturation and then supersaturation of the vapor. It is of interest to determine how the increase in supersaturation is affected by the occurrence of a non-isentropic process at some stage of the expansion. In particular, it is desired to determine the effect of a shock wave on the supersaturation of water vapor in air that is being expanded isentropically in a supersonic nozzle.

Considering the one-dimensional shock case, it follows immediately from the equations for the conservation of mass, momentum and energy across a normal shock (equations (I.1), (I.2) and (I.3) of Appendix I, for $\dot{q} = 0$) that

$$(p_1 - p_2)\left(\frac{1}{\rho_1} + \frac{1}{\rho_2}\right) = \frac{2\gamma'}{\gamma' - 1}\left(\frac{p_1}{\rho_1} - \frac{p_2}{\rho_2}\right)$$

* See equation (I.11), Appendix I.

where subscripts 1 and 2 refer to conditions immediately in front of and behind the shock, respectively, and γ' is the ratio of the specific heats for the mixture of water vapor and dry air.

Utilizing the perfect gas law, this equation can be written in the form

$$(p_1 - p_2)\left(\frac{1}{\rho_1} + \frac{1}{\rho_2}\right) = \frac{2\gamma'}{\gamma' - 1}\,\frac{R}{m}\,(T_1 - T_2)$$

or,

$$\frac{\Delta p}{\Delta T} = c_p\,\rho_1 \cdot \frac{2}{1 + \frac{\rho_1}{\rho_2}} \tag{2.14}$$

Since the preceding equations refer to the mixture of water vapor and dry air, it will be necessary to use some of the relationships of the preceding section between the water vapor and the mixture in order to arrive at an equation that can be compared with the Clausius-Clapeyron relation.

Thus, from equation (2.7),

$$\frac{\Delta p_v}{p_{v_1}} = \frac{\Delta p}{p_1}$$

Moreover,

$$c_p = \frac{c_{p_a} + \chi c_{p_v}}{1 + \chi} = c_{p_v} \cdot \frac{\frac{c_{p_a}}{c_{p_v}} + \chi}{1 + \chi}$$

and

$$\frac{R}{m} = R\,\frac{\left(\frac{1}{m_a} + \frac{\chi}{m_v}\right)}{1 + \chi} = \frac{R}{m_v}\,\frac{(\epsilon + \chi)}{1 + \chi}$$

Hence, equation (2.14) becomes

$$\frac{\Delta p_v}{\Delta T} = c_p \frac{p_{v_1}}{\frac{R}{m} T_1} \cdot \frac{2}{1+\frac{\rho_1}{\rho_2}} = c_{p_v} \cdot \frac{p_{v_1}}{\frac{R}{m_v} T_1} \cdot \frac{\frac{c_{p_a}}{c_{p_v}} + \varkappa}{\varepsilon + \varkappa} \cdot \frac{2}{1+\frac{\rho_1}{\rho_2}} \qquad (2.15)$$

The change in the saturation vapor pressure across the shock is given by the Clausius-Clapeyron equation (2.13) in the form

$$\frac{\Delta p_{v_\infty}}{\Delta T} = \frac{L_1}{T_1} \frac{p_{v_1}}{\frac{R}{m_v} T_1} \qquad (2.13a)$$

Comparing equation (2.13a) with (2.15), it is apparent that the supersaturation is decreased in passing through the shock as long as the temperature before the shock is less than 550° K., since, below this temperature, $\frac{L_1}{T_1} > c_{p_v} \cdot \frac{c_{p_a}/c_{p_v} + \varkappa}{\varepsilon + \varkappa} \cdot \frac{2}{1 + \rho_1/\rho_2}$, regardless of the strength of the shock.

C. Equilibrium Between a Liquid Drop and its Vapor

In order to obtain an understanding of the mechanism whereby a supersaturated vapor may exist in a stable, or more precisely a metastable, state and whereby it may collapse with the attendant formation of liquid droplets, it is necessary to consider the equilibrium between a liquid drop and its supersaturated vapor.

Consider an heterogeneous system consisting of the vapor phase (denoted by subscript v), the liquid phase (denoted by subscript ℓ) and a surface of discontinuity separating these two phases. The state of each phase may be specified by its volume, V, its entropy, S, and, to allow for the transfer of mass from one phase into the other, the

mass of the substance, n, measured in moles.

The primary condition for thermodynamic equilibrium between the vapor phase and the liquid phase is that the variation of the total internal energy vanish for all possible virtual changes of the parameters of the system (see, e.g. Epstein [18]). The internal energy, being an extensive property, is the sum of the internal energy of each phase and the energy associated with the surface of discontinuity separating them, which is a function of the area and curvature of the surface.

Therefore,

$$\delta E = T_v\,\delta S_v + T_\ell\,\delta S_\ell - p_v\,\delta V_v - p_\ell\,\delta V_\ell$$

$$+ \phi_v\,\delta n_v + \phi_\ell\,\delta n_\ell + \sigma\,\delta\Sigma + C\,\delta c = 0 \qquad (2.16)$$

is the condition for equilibrium between a liquid droplet and its vapor, where ϕ is the molar thermodynamic potential, σ the surface tension, Σ the area and c the curvature of the surface.

Gibbs [19] has shown that the surface of discontinuity can be located in such a way that $C = 0$ and still retain its physical significance. He calls this surface the "Surface of Tension".

Consider, now, the following three possible variations:

a) $\qquad \delta S_v = -\delta S_\ell \;;\; \delta V_v = \delta V_\ell = \delta n_v = \delta n_\ell = \delta\Sigma = 0$

then equation (2.16) becomes

$$\delta E = (T_v - T_\ell)\,\delta S_v = 0$$

or

$$T_v = T_\ell \tag{2.17}$$

Hence, in thermodynamic equilibrium, the temperature is uniform throughout.

b) $\delta V_v = -\delta V_\ell$, $\delta \Sigma \neq 0$; $\delta S_v = \delta S_\ell = \delta n_v = \delta n_\ell = 0$

then,

$$\delta E = (p_v - p_\ell)\, \delta V_\ell + \sigma \delta \Sigma = 0$$

$$\therefore \quad p_\ell - p_v = \sigma \frac{\delta \Sigma}{\delta V_\ell} \tag{2.18}$$

And, if the liquid phase is assumed to be a spherical droplet, equation (2.18) becomes

$$p_\ell - p_v = \sigma \cdot \frac{8\pi r \delta r}{4\pi r^2 \delta r} = 2\frac{\sigma}{r} \tag{2.19}$$

Thus, the pressure within the liquid droplet is greater than that of the vapor by the amount $2\frac{\sigma}{r}$. Equation (2.19) was first developed by Lord Kelvin from mechanical considerations and is generally referred to in his name.

a) $\delta n_v = -\delta n_\ell$; $\delta S_v = \delta S_\ell = \delta V_v = \delta V_\ell = \delta \Sigma = 0$

then,

$$\delta E = (\phi_v - \phi_\ell)\, \delta n_v = 0$$

whence,

$$\phi_v = \phi_\ell \tag{2.20}$$

Thus, when the free transport of mass is allowed, the molar thermodynamic potential is uniform throughout.

In the case of chemically pure phases, as considered herein, $\phi = \frac{F}{n}$ and is independent of n.

Hence,

$$d\phi = \frac{dF}{n} = -\frac{S}{n} dT + \frac{V}{n} dp \tag{2.21}$$

At constant temperature, equation (2.21) becomes

$$\upsilon_v\, dp_v = \upsilon_\ell\, dp_\ell \qquad \text{where } \upsilon = \frac{V}{n}$$

or

$$\frac{RT}{p_v} dp_v = \upsilon_\ell\, dp_\ell$$

Integrating, with the assumption that the liquid phase is incompressible (υ_ℓ = constant):

$$RT \ln \frac{p_v}{p_\infty} = \upsilon_\ell (p_\ell - p_\infty)$$

or,

$$\ln \frac{p_v}{p_\infty} = \frac{\upsilon_\ell}{RT} (p_\ell - p_\infty) = \frac{\upsilon_\ell}{RT} \left[(p_\ell - p_v) + (p_v - p_\infty) \right] \tag{2.22}$$

where, p_∞ is the saturation vapor pressure corresponding to a droplet of infinite radius, i.e., a plane surface of water. Utilizing equation (2.19) in (2.22):

$$\ln \frac{p_v}{p_\infty} = \frac{v_l}{RT}\left[2\frac{\sigma}{r} + (p_v - p_\infty)\right] \qquad (2.23)$$

Since $(p_v - p_\infty)$ is normally negligible in comparison with $2\frac{\sigma}{r}$, equation (2.23) reduces to the familiar Thomson-Gibbs equation,

$$\ln \frac{p_v}{p_\infty} = \frac{v_l}{RT} \cdot \frac{2\sigma}{r} = \frac{m_l}{\rho_l RT} \cdot \frac{2\sigma}{r} \qquad (2.24)$$

Equation (2.24) is valid provided $r > 10^{-6}$ cm., since it has been implicitly assumed in the derivation of equation(2.24) that the surface tension is independent of r, which is true only for values of r above this approximate value. A plot of equation (2.24) in the form of p_v/p_∞ vs. r for various values of T is shown in Fig. 3, both for the case where σ is considered independent of r and where the dependence on r, as developed by Tolman (see Fig. 16), is taken into account.

Thus at room temperatures, it is not until the droplet becomes of the order of the wave-length of visible light and smaller that the effects of curvature on the saturation vapor pressure becomes important. The effect of decreasing temperature, however, is such as to increase the ratio p_v/p_∞ for a given size droplet, inasmuch as σ /T increases with decreasing temperature. Conversely, for a given supersaturation ratio, the size required of a droplet in order for it to be in equilibrium increases as the temperature decreases.

It will be seen in Part IV that the value attained by the supersaturation ratio is, in some cases, so large that the radius as determined by the Thomson-Gibbs equation, assuming the extrapolation of σ to low temperatures is correct, is of the order of 10^{-8} cm. Since this value is of the order of the radius of a water vapor molecule, the medium has long since ceased to be a continuum and hence the equation has no significance.

D. The Spontaneous Formation of Liquid Droplets or Ice Particles

It was seen in the preceding section that for a given supersaturation, P_v/P_∞, there corresponds a particular droplet of characteristic radius, r*, such that for $r < r^*$ the droplet vaporizes and for $r > r^*$ the droplet grows. It has been shown that the effects of foreign nuclei and ions are negligible in the case of condensation in wind tunnels and that, even in the absence of such nuclei, condensation occurs in the Wilson Cloud Chamber. Hence, the origin of condensation must be found here in fluctuations and a statistical approach must therefore be used to determine the probability of formation of droplets of the characteristic radius. This method of approach was first used by Volmer [20] and reference should be made to his work for a more detailed analysis.

The probability, P, for the formation of the characteristic radius droplet is given by Boltzmann's principle

$$P = A \cdot e^{-\frac{\Delta W}{kT}} \qquad (2.25)$$

where, ΔW is the work of formation of the droplet

k = Boltzmann's constant

A = constant of proportionality

The total work of formation is the difference between the work done against the surface tension and the work done by the pressure forces. The area of the droplet increases from 0 to $4\pi r^{*2}$ while the volume increases from 0 to $4/3\ \pi r^{*3}$, hence, the work done against the surface tension is

$$.4\pi r^{*2} \cdot \sigma$$

and the work done by the pressure forces is

$$(P_l - P_v)\frac{4}{3}\pi r^{*3}$$

or, using the Kelvin relation,

$$P_l - P_v = \frac{2\sigma}{r^*} \qquad (2.19)$$

this work release becomes

$$\frac{2}{3} \times 4\pi r^{*2}\sigma$$

Whence, the total work of formation of the droplet is

$$\Delta W = \frac{4\pi r^{*2}\sigma}{3} \qquad (2.26)$$

Since the frequency of formation, J, of droplets of the characteristic size is proportional to the probability, P, J is given by

$$J = K \cdot e^{-\frac{\Delta W}{kT}} = K \cdot e^{-\frac{4\pi r^{*2}\sigma}{3kT}} \qquad (2.27)$$

or, using the Thomson-Gibbs relation, equation (2.24)

$$J = K \cdot e^{-\frac{16\pi\sigma^3 m_v^2 N_o}{3R^3T^3\rho^2\left(\ln P_v/P_\infty\right)^2}} \qquad (2.28)$$

where,

m_v = molecular weight of the vapor

N_o = Avogadro's number = 6.023×10^{23} molecules/mole

R = Universal gas constant = 8.315×10^7 ergs/mole/° K.

ρ_l = density of the liquid phase

P_v/P_∞ = supersaturation ratio.

Since the Thomson-Gibbs equation was utilized in arriving at the final equation for the nuclei formation frequency, equation (2.28), it was implicitly assumed that thermal equilibrium is maintained during the formation of the droplets, i.e., that the necessary transport of the latent heat of vaporization away from the surface of the droplet is provided for in order that the droplet temperature be equal to the temperature of the surrounding medium. It is evident that if the temperature of the droplet of characteristic radius is higher than that of the vapor, the droplet will vaporize, since in this case, a higher vapor pressure is required in order for the droplet to be stable.

The considerations utilized in obtaining equation (2.28) leave the constant of proportionality, K, undetermined. Several investigators have attempted to improve upon Volmer's derivation. A few of the attempts are considered in the next paragraph. None of them, however, can be said

to be adequate since all of them essentially treat the process as stationary, a condition which is not well satisfied in practice.

E. Kinetic Considerations

The determination of the constant of proportionality, K, in the nuclei formation frequency equation has been attacked by slightly different methods by a number of authors, including Zeldovich [21], Becker and Döring [22], Volmer* and Weber [23], Farkas [24] and Stranski and Kaischew [25]. Frenkel [26] includes a very satisfactory development of Volmer's approximate equation and presents Zeldovich's method of obtaining an approximate solution to the Becker-Döring equation. Charyk* has presented Becker and Döring's method of attack and, therefrom, has determined the relationship between the threshold supersaturation ratio and the temperature for an assumed value for J of 1,000.

No attempt will be made here to present any of the above-mentioned methods in detail. Instead, only the fundamental approach, the basic assumptions and the final results will be considered.

In all cases, the concept of a quasi-stationary phase transition process is utilized in which, through the purely statistical collision of the vapor molecules, droplets are assumed to form and grow continually in a supersaturated vapor contained in a large vessel. The vapor is maintained in a stationary state by eliminating from the system droplets which have reached a certain size G larger than that of a droplet g* of characteristic radius and replacing them by an equivalent number of single molecules GN_G, where G is the number of molecules in a droplet

---

* loc. cit.

of maximum allowed size and N_G is the number of such droplets.

In addition, Volmer assumes that the rate of growth of all the droplets of various sizes is proportional to the total number of droplets of characteristic radius, N_{g^*}, existing in the vapor at any given instant and that the rate of formation of these latter droplets is then given by the product of the number of such droplets and the number of single molecules of the vapor, β, that strike their surface in unit time.

An expression for the total number of droplets of characteristic radius is obtained by considering the change in the thermodynamic potential of the system when a transition of a given number of molecules of the vapor phase into a nucleus of the liquid phase occurs and then treating the nuclei as the solutes of a "dilute solution", the vapor phase being the solvent:

$$N_{g^*} = N \cdot e^{-\frac{4\pi r^{*2}\sigma}{3kT}} \tag{2.29}$$

where, g^* = number of molecules in a nucleus of characteristic radius, r^*

N = total number of molecules in the system

$$= N_1 + \sum_{g=2}^{G} g N_g$$

N_1 = total number of vapor molecules.

This same equation can be obtained more easily from a consideration of Boltzmann's principle, equation (2.25), and the work required to form

a droplet of characteristic radius, equation (2.26). Thus,

$$N_g = C \cdot e^{-\frac{\Delta W_r}{kT}} \tag{2.30}$$

whence,

$$N_g^* = N \cdot e^{-\frac{4\pi r^{*2}\sigma}{3kT}} \tag{2.29}$$

where the constant of proportionality, C, is equal to the total number of molecules in the system, N, as long as the number of nuclei is small compared with the total number of vapor molecules. Equation (2.30), however, determines an equilibrium distribution of the nuclei with respect to their size, which is essentially equivalent to Volmer's consideration.

From kinetic theory considerations, the number of single molecules striking the surface of these droplets in unit time and per unit area is determined as

$$\beta = \frac{p}{\sqrt{2\pi m k T}} \tag{2.31}$$

where, p is the pressure and m the molecular weight.

Hence, the Volmer theory gives, as the equation for the nuclei formation frequency:

$$J = N_g^* \cdot 4\pi r^{*2} \beta = N \cdot (4\pi r^{*2}) \frac{p}{\sqrt{2\pi m k T}} \cdot e^{-\frac{4\pi r^{*2}\sigma}{3kT}} \tag{2.32}$$

Becker and Döring, on the other hand, derive the nuclei formation frequency from purely kinetic considerations, rejecting the thermodynamic considerations of Volmer but retaining the assumption of a quasi-stationary state. In addition, they take into account the evaporation from the surface of the drops as well as the process of condensation.

For an equilibrium distribution of droplets with respect to their size, the following equation is valid:

$$N_g S_g \alpha_g = N_{g-1} S_{g-1} \beta \qquad (2.33)$$

where N_g and N_{g-1} are the number of droplets containing g and (g-1) molecules, respectively.

S is the corresponding surface area of the droplet.

α_g is the probability that one molecule leaves a unit surface area of a droplet containing g molecules.

β is the probability that one molecule condenses on a unit surface area.

Hence, denoting the number of droplets containing g molecules under a non-equilibrium distribution by f_g:

$$f_{g-1} S_{g-1} \beta - f_g S_g \alpha_g = J_g \neq 0 \qquad (2.34)$$

Thus, J_g represents the increase in the class (g) due to condensation of the vapor on the surface of droplets in class (g-1), or the increase in the class (g-1) due to evaporation of the droplets in class (g).

From equations (2.33) and (2.34), the rate of change of the number of droplets in a given class is found to be

$$\frac{\partial f_g}{\partial t} = J_g - J_{g+1} \tag{2.35}$$

Becker and Döring then solve equation (2.35) assuming a) a steady distribution in size, i.e., $\partial f_g / \partial t = 0$ and hence J = constant, and b) that β is the average rate at which a molecule joins the droplet under equilibrium conditions. These additional assumptions, together with the boundary condition $f_G = 0$, where G is the maximum-allowed size ($G > g^*$), determine a set of algebraic equations which they solve by means of an electrical analogy (see also Charyk for details).

The result then obtained is

$$J = \frac{\beta N_1 S_1}{3g^*} \sqrt{\frac{4\pi r^{*2}\sigma}{\pi k T}} \cdot e^{-\frac{4\pi r^{*2}\sigma}{3kT}} \tag{2.36}$$

Or, with the aid of the Thomson-Gibbs equation (2.24):

$$J = \frac{\beta N_1 S_1}{3g^*} \sqrt{\frac{4\pi r^{*2}\sigma}{\pi k T}}\; e^{-\frac{16\pi m^2 N_0 \sigma^3}{3R^3 T^3 \rho_l^2 \left(\ln \rho_v/\rho_\infty\right)^2}} \tag{2.37}$$

where, $N_1 S_1$ is the total surface area of the single molecules and g^* is given by

$$g^* = \frac{4}{3}\pi r^{*3}\frac{\rho N_0}{m}$$

From kinetic theory considerations, the quantity ($\beta N_1 S_1$) is evaluated as

$$\beta N_1 S_1 = N_0 \sqrt{\frac{8}{\pi R}} \cdot \frac{T_0}{p_0 l_0} \cdot \frac{1}{\sqrt{m}} \cdot \frac{p^2}{T^{3/2}}$$

where, N_o = Avogadro's number = 6.023×10^{23} molecules/mole

R = Universal gas constant = 8.31×10^{7} ergs/°K./mole

ℓ_o = mean free path at S.T.P.

or,

$$\beta N_1 S_1 = 5.05 \times 10^{22} \frac{P_\infty^2}{\ell_o \sqrt{m}\, T^{3/2}} \left(\frac{P}{P_\infty}\right)^2$$

if p is expressed in millimeters of mercury.

Zeldovich solves the Becker-Döring equation, under the same assumption of a steady distribution, i.e., J = constant, by an approximate method that is much simpler and more straightforward than that used by Becker and Döring and arrives at a final equation for the nuclei formation frequency that is almost identical to that of these authors.

Even though the Becker-Döring equation for the nuclei formation frequency can be considered to be the most accurate one to-date, under the assumptions involved, for describing the spontaneous condensation process, it will be seen in the next section that serious limitations exist with regard to the application of this equation to the problem of condensation in wind tunnels.

F. Limitations of Existing Theories

The theories discussed in the preceding section have the following limitations when considered in the light of spontaneous condensation in supersonic wind tunnels:

1) The rapidity of the expansion results in marked deviations from the quasi-stationary condition. Hence the solutions are not adequate and a time-dependent solution of the basic Becker-Doring equation is actually necessary.

2) The degree of supersaturation attained prior to the collapse of the supersaturated state is so high that the number of molecules in the characteristic-size droplet becomes of the order of ten or less. In this case there is no justification for considering "g" a continuous variable and replacing the difference equation by a differential equation.

3) For such small droplets, the variation of the surface tension with droplet radius must be taken into account in the Thomson-Gibbs equation. Tolman[27] arrived at such a relationship from a consideration of Gibbs theory of surface tension and the result, as applied to water droplets, is shown in Fig. 16.

4) The temperature at which condensation occurs is normally well below 0° C., in which region no data exist on the surface tension of water, even for large droplets, and hence an extrapolation must be made. The variation of surface tension with temperature, as obtained from the International Critical Tables [23], together with the questionable extrapolation to temperatures below 0° C., is presented in Fig. 15.

5) The effect of the rate of growth of droplets on the surface tension is unknown.

The surface tension is particularly troublesome in the nuclei formation frequency equation since, as can be seen from equ. (2.37), it appears to the third power in the exponent and hence a small error

in the surface tension can result in an appreciable error in J. One favorable result in this regard, however, is the fact that, with decreasing temperature, the error in J decreases for a given error in σ . This is illustrated in Fig. 4, where the variation in the error of J with temperature is presented for an error in σ of 10%, i.e. $\sigma'/\sigma = 1.10$. Even at the lower temperatures it is seen that a 100% error in J can result.

These latter considerations show that the application of the theory to the formation of ice particles, rather than water droplets, cannot be made at this time in view of the lack of data on the surface energy of ice. For this reason the theoretical discussion included herein deals only with the formation of liquid droplets.

PART III

EXPERIMENTAL TECHNIQUES

Numerous different experimental techniques were utilized in an effort to determine the location of the collapse of the supersaturated state, the intensity of this collapse, the resulting size and concentration of droplets and the subsequent growth of these droplets, when humid air is expanded in a wind tunnel. Since some of the techniques most useful for such measurements may be new to investigators in the field, a brief description of them is believed to be worthwhile, even though the full potentialities have not been realized in some cases. Additional techniques that may be applicable in some instances, but which were not used extensively in this investigation, are discussed briefly in Appendix IV.

A. Pressure Measurements

The simplest and most logical method for accurately determining the location and intensity of the collapse of the supersaturated state in a wind tunnel is by means of static pressure measurements. This is due to the fact that the sudden release of heat, resulting from the spontaneous condensation, causes the flow parameters to deviate from their isentropic values at that point. Hence, for given stagnation conditions, the location of the collapse is obtained from axial static pressure distribution measurements as that point at which the ratio p/p_o starts diverging from the corresponding isentropic curve. A similar method is to continuously decrease the stagnation relative

humidity by raising the stagnation temperature and observing the change in p/p_o at one location in the nozzle as the condensation region moves past it. This technique, however, may give misleading results, as will be pointed out in Part VI.

The intensity of the collapse is determined, in these two techniques, by the magnitude of the divergence from the isentropic curve immediately after the collapse has taken place, i.e., the intensity is measured by the ratio p_o/p_o', which is obtained from the pressure distribution measurements by taking the ratio of p/p_o' immediately after the collapse (point "C" in Fig. 6a) to $(p/p_o)_{isentropic}$ corresponding to the same point in the tunnel (point "E" in Fig. 6a).

The droplet growth can be determined from the change in p_o/p_o' downstream of the region of collapse provided this growth is at the expense of the vapor and not of the smaller droplets.

The intensity of collapse can also be determined by measuring p_o' directly by means of a total head tube. However, in this case, account must be taken of the change in stagnation pressure across the detached shock associated with the probe.

B. Optical Methods

1. Schlieren

The location of the start of spontaneous condensation can be determined with fair accuracy by means of Schlieren observations in those cases where the heat release is sudden enough and of such a magnitude as to cause a sharp "condensation shock".

The experiments to be discussed in the next chapter have shown that under such conditions the location as observed in the Schlieren and that determined from pressure distribution measurements are in very good agreement. From a knowledge of the area ratio at that station in the nozzle observed in the Schlieren, the pressure ratio, etc., immediately prior to condensation can be calculated directly.

The "condensation shocks" observed during the course of this experimental program, together with those of Hermann and the NACA, tend to confirm the fact that the so-called "X-shocks" occur in rapidly diverging nozzles, while normal or slightly curved condensation shocks occur in slowly diverging ones. This is to be expected in view of the fact that the flow parameters are not constant over a cross-section of a rapidly diverging nozzle, and thus the condensation takes place at the wall first, where the expansion is the greatest. However, it is still not clear whether the condensation occurring at the wall creates a disturbance that is propogated downstream in the form of the X-shock or whether the collapse takes place across the nozzle in such a form. In addition, there may be secondary effects, such as boundary layer separation immediately downstream of the region of intense condensation, that further complicate the problem.

Schlieren observations of the shock wave attached to a cone or wedge of known angle can also be utilized to obtain quantitative information on the condensation process, such as the change in Mach number with change in water vapor content, but this technique

has limited accuracy, and may give incorrect results (see Part VII,B).

At very low densities the Schlieren method loses its utility since the shock waves become so weak as to be barely discernible, while with little or continuous heat addition a shock wave of finite strength does not exist.

2. Rayleigh Light Scattering

When a monochromatic light of given intensity traverses a medium containing particles whose linear dimensions are small compared with the wave-length of the light, the well-known phenomenon of light scattering takes place, the intensity of the scattered light being given by the equation due to Lord Rayleigh (29),

$$\frac{I_\beta}{I_o} = \frac{(\rho' - \rho)^2}{\rho^2} (1 + \cos^2 \beta) \frac{n \pi V^2}{\lambda^4 d^2} \qquad (3.1)$$

where,

I_β = intensity of the scattered light observed at an angle β to the incident light

I_o = intensity of the incident light

ρ' = density of the particles

ρ = density of the medium

n = number of particles

V = volume of the particles

λ = wave-length of the monochromatic light

d = distance of the observer from the particles.

The light scattering technique is probably the simplest method for qualitatively observing condensation in wind tunnels, since the intensity of light scattered by the droplets is very

high, while the humid air immediately upstream of the condensation exhibits no observable scattering whatsoever. Hence, the location of the start of condensation is readily discernible and agrees with that determined by pressure distribution measurements within the accuracy of the technique (about $\pm$ 1 mm.). This accuracy can be increased somewhat by using a Nicol prism or Polaroid lens and observing the appearance and disappearance of the scattered light as the prism is rotated about the null point. This appearance and disappearance takes place when the scattered light, as in pure Rayleigh scattering, is plane polarized. If the linear dimensions of the particles are not small in comparison with the wave-length, the scattered light will not be plane polarized; in fact in this case ordinary diffuse reflection from the surface of the particles and not true scattering results.

In all of the light scattering observations of the start of condensation undertaken in this investigation, the scattered light was found to be plane polarized and, moreover, was found to be blue when white incident light was used. Both of these facts lead to the conclusion that the droplets are small enough for the Rayleigh scattering formula to be valid. Hence, even though this equation cannot be solved for the number or size of droplets uniquely, it will be possible to set some upper and lower bounds on these values, at least as to order of magnitude:

Assuming $d = 10$ cm. and $\lambda = 0.48 \times 10^{-4}$ cm. and taking $\rho \doteq 10^{-3}$ gm./cm^3., equation (3.1) becomes approximately:

$$\frac{I_{90^\circ}}{I_o} = \left(\frac{\rho'}{\rho} - 1\right)^2 \frac{\pi (4/3\pi)^2 \cdot nr^6}{\lambda^4 d^2} \doteq 10^{23}\, nr^6$$

when the observer is normal to the incident light.

If the Rayleigh equation holds for droplets up to 10^{-6} cm. in radius (the linear dimension of the droplet corresponding to about 0.04 λ) then, for $0.1 < I_\beta/I_o < 1.0$,

$$10^{12} < n < 10^{13}$$

which represents an approximate lower bound for the number of droplets.

The maximum number of droplets is obtained when the "droplet" contains only one molecule. Using the radius of the water vapor molecule as calculated from Van der Waals' equation, $r \doteq 1.4 \times 10^{-8}$ cm., the following upper limit is obtained:

for $0.1 < I_\beta/I_o < 1.0$, $\quad 10^{23} < n < 10^{24}$

Since, from a measurement of the intensity of the incident and scattered light, the product nr^6 can be determined, it will be possible to determine the average radius of the droplets fairly accurately if some other technique determines the product nr^α, where α is some power other than the sixth. Such a technique is that of measuring the pressure distribution, inasmuch as the departure from the isentropic curve is proportional to the amount of water vapor condensed out of the system, from which the product nr^3 can be obtained. The ratio of the values given by these two different techniques determines r^3, and hence the error in r will be relatively small.

A technique that has been found to be of value in

determining the relative intensities of the incident and the scattered light is that of separately photographing each one at the same exposure time and thence making microphotometer traces from the negatives. In the present investigation, however, the intensity of the scattered light in the Laval nozzle tests was too low to enable proper photographs to be taken.

PART IV

MEASUREMENTS OF THE COLLAPSE OF THE SUPERSATURATED STATE

A. Apparatus

The present series of experiments was performed mainly in a small Laval nozzle and in the GALCIT 2.5" x 2.5" supersonic and 4" x 10", nee 2" x 20", transonic wind tunnels. In addition, Mr. A. E. Puckett has generously furnished valuable data from the J. P. L. 12" x 12" supersonic wind tunnel and some preliminary results from the GALCIT hypersonic wind tunnel.

The Laval nozzle was a two-dimensional, straight-sided, symmetrical nozzle of rectangular cross-section. The straight diverging walls had an included angle of 4 $^{\circ}$ and were faired into the throat by means of a large arbitrary radius. The other two walls were both of plate glass, when optical measurements were being made, while one of these was replaced by a metal plate containing axially distributed static pressure holes for the pressure distribution measurements.

In order to facilitate light scattering observations, the nozzle blocks were made of Lucite, the flat sides of which were painted with optical black paint. The incident light could then be directed through one of the nozzle blocks and the scattered light observed at an angle of 90° through one of the glass walls. This technique possessed the additional advantage that the incident light could be focused at a particular location in the nozzle by means of suitable lenses.

Humid air from the building compressed air supply was introduced, through a quick-opening valve, into the stagnation chamber and thence through the nozzle into the atmosphere (see Fig. 5). The stagnation temperature was measured by means of a thermocouple and a self-balancing potentiometer; while the stagnation pressure, because of its high value, was measured with a standard pressure gage. The dew point was measured by conducting a small amount of the air in the stagnation chamber through a chamber housing a carbon-dioxide-cooled mirror to the atmosphere. The pressure in the dew point indicator was measured in order that, with the measured value of the dew point, the actual partial pressure of the water vapor under stagnation conditions could be determined. (See Appendix II for sample calculations).

The stagnation relative humidity of the air has been found to be the main parameter that determines where the collapse of the supersaturated state is to occur. This quantity is varied in the Laval nozzle tests simply by changing the stagnation pressure, inasmuch as the partial pressure of the water vapor varies directly with the air pressure and hence, also, for a constant stagnation temperature, does the stagnation relative humidity, $(p_v/p_\infty)_o$.

It was found in the light scattering tests in the Laval nozzle that, as the stagnation pressure was increased from 10 psig to the maximum available pressure of 50 psig, the location of the start of condensation moved upstream about one-half an inch. Therefore, for the pressure distribution measurements, the static pressure holes,

of about 0.0135" diameter, were axially located in the steel plate at 1/8" intervals over a range of 1-3/8" and so situated as to bracket the movement of the start of condensation. Downstream of this region a greater interval was used. The pressures were indicated on a mercury manometer, which could be read with an accuracy of about $\pm$ 0.1 mm. Hg.

In addition to the light scattering and pressure distribution measurements, Schlieren observations were made and the diffraction ring technique, discussed in Appendix IV, was investigated.

The GALCIT 2 1/2" x 2 1/2" supersonic wind tunnel is of the closed-return type with plate glass side walls and interchangeable nozzle blocks, designed for Mach numbers of 1.6, 2.0, 3.2 and 4.4, comprising the top and bottom walls. In addition there was an adjustable nozzle that could cover the Mach number range from 1.2 to 2.0. The stagnation conditions were measured in the same manner as in the Laval nozzle tests with the exception of the stagnation pressure, which could be read on a manometer.

For all of these Mach numbers, the procedure of recording the static pressure at some location in the test section, as the initial relative humidity was decreased step-by-step, was used. This decrease in relative humidity was accomplished by drying the air in successive stages until no change could be observed in the static pressure.

For the lower Mach number tests, up to and including 2.0, additional investigations were made by taking a static pressure

survey from the droplet-free air through and downstream of the region of condensation. Due to the lack of static pressure holes along the side walls of the tunnel, a long metal tube that completely spanned the length of the nozzle blocks was located on the axis of the tunnel. This tube was supported at one end by the sting in the test section and at the other by a strut located in the extreme forward part of the subsonic section. A single static pressure hole was drilled normal to the axis of the tube at such a location that the pressure distribution through the condensation region could be determined by movement of the tube as a whole. The static pressure at each location of the static hole was then measured by means of a manometer, while the stagnation conditions were held constant.

Schlieren observations were made concurrently during these investigations, as were light scattering observations. For the latter, however, the solid metal nozzle blocks necessitated using the relatively crude technique of shining a light through the glass side walls at as acute an angle to the axis of the tunnel as could be achieved and observing the light scattered normal to the axis. Nevertheless, this procedure sufficed as far as qualitative observations were concerned, since the start of condensation and its progression downstream were very distinct.

The GALCIT 4" x 10" Transonic Wind Tunnel is also of the closed return type, but has several advantages over the 2.5" x 2.5" Supersonic Wind Tunnel that make it very well suited for the in-

vestigation of condensation phenomena: a) a flexible nozzle comprises the bottom wall of the nozzle, while the top wall is straight and hence is essentially the central streamline of a tunnel of twice the height; thus a comparison between the data from this tunnel and that from the Laval nozzle tests is of value in determining the effect of scale on the condensation phenomena, b) the Schlieren windows are removable and can be replaced with plates containing closely spaced static pressure holes for pressure distribution measurements and c) the stagnation temperature can be varied over a wide range which, in conjunction with the wind tunnel dryer, allowed a wide variety of initial relative and specific humidities to be obtained.

Prior to its redesign into the present 4" x 10" cross-section, the Transonic Wind Tunnel had a 2" x 20" test section and provisions for mounting various two-dimensional airfoil sections between the two Schlieren windows. Although no measurements were made at that time of the start of condensation, numerous light scattering and Schlieren photographs were taken of the flow over a 12% thick, bi-convex airfoil when condensation was present. For these investigations, a Lucite window was fashioned into the top nozzle block, through which the light from two photoflood lamps passed into the test section. The scattered light was then photographed through one of the Schlieren windows on the side wall. Schlieren and light scattering pictures could thus be taken within a very short time of one another. The results of these investigations are discussed in Part VIII.

B. Results and Discussion

The results of the pressure distribution measurements obtained from the Laval nozzle tests are plotted in Figures 6a, b, and c in the form of p/p_o vs. the axial distance along the nozzle measured from an arbitrary section upstream of the throat. The isentropic curve as calculated from the area-ratio is shown, also, together with the pressure distribution as measured from tests using commercially dry nitrogen. (It should be pointed out that, as was found in this investigation, even the commercially obtainable "dry" nitrogen contains a sufficient amount of water vapor as to result in condensation occurring at high Mach numbers.) It is readily apparent from these curves that the location of the collapse of the supersaturated state moves downstream as the initial relative humidity decreases; i.e., as p_o decreases. Since the water vapor content, as expressed by either the mixing ratio or the specific humidity, remained practically constant throughout this series of tests, it is to be expected that the intensity of the collapse, i.e. the total amount of water vapor condensed out in the process, would be the same in all cases. This expectation is not borne out in the present investigations, as an examination of Fig. 6 shows. It is seen that the intensity of the collapse continually decreases as the initial relative humidity is decreased. This is apparently due to a continual increase in condensation prior to the final collapse, as illustrated by the continual divergence from the isentropic

curve. The calculations in Appendix III show that, for the low mixing ratios present in these tests (about 3×10^{-3} gms/gm), the isentropic curve for dry air is practically coincident with that for humid air and hence the pronounced divergence of the humid air curves from the isentropic cannot be due to neglecting the effect of the presence of the vapor.

The total amount of water vapor condensed out of the system, i.e., including the condensation prior to collapse as well as that at the collapse, is evidently nearly the same in all cases, since all of the curves approach each other downstream of the collapse. Hence, it is concluded that, for a given nozzle, the total amount of water vapor condensed out depends only upon the water vapor content of the air, whereas the location of the collapse depends only upon the initial relative humidity.

If the location of the collapse of the supersaturated state is determined as that location in the nozzle where the pressure commences to increase suddenly, then the supersaturation ratio at that point, the so-called "threshold supersaturation ratio", can be calculated (see Appendix II for computational procedures) under the assumption that the flow is isentropic up to that point. These calculations are presented in the form of the natural logarithm of the threshold supersaturation ratio vs. the local temperature, (Fig. 1).

Representative pressure distribution curves obtained from the 2 1/2" Supersonic Wind Tunnel, by means of the static pressure probe, and the 4" x 10" Transonic Wind Tunnel, utilizing the pressure

distribution plate, are presented in Figures 7a and 7b, resp. Calculations were made of the threshold supersaturation ratios in these cases, also, and the results presented in Fig. 1.

In those instances where the static pressure was observed at one location in the wind tunnel as the initial relative humidity was decreased, the static pressure was seen to decrease until the region of condensation had moved downstream of the static hole, whereupon it remained constant. A typical pressure curve obtained in this manner is shown in Figure 8. Here, again, the threshold supersaturation ratio, corresponding to that point at which the pressure starts increasing, is calculated.

The pressure data obtained by the NACA, Oswatitsch, Redington and Binnie and Woods * has been used to calculate the threshhld supersaturation ratios in these cases, in order that a comparison between all the available data could be made. These results are similarly plotted in Fig. 1.

An examination of this figure apparently shows considerable scatter among the various experimental points. However, when considered in the light of the dynamical effects, to be discussed in the next section, the scatter is no greater than would be expected on the basis of experimental errors and the fact that, in many instances, the location of the collapse of the supersaturated state could not be determined accurately. In fact, in a number of cases, the collapse took place in a gradual manner with the result

* loc. cit.

that the determination of the threshold supersaturation ratio becomes much more arbitrary.

PART V

DYNAMIC EFFECTS

It is to be expected that, when the theory is applied to the flow in a supersonic nozzle, the utilization of the quasi-stationary hypothesis will result in a conservative determination for the value of the supersaturation ratio, at a given temperature, at which the collapse of the supersaturated state occurs. This expectation is based on the fact that the vapor is not in a stationary state, as assumed in the theory, but is continually increasing in its degree of supersaturation as it expands. Hence a time lag, between the point at which the collapse is theoretically predicted and where it actually occurs, must result which depends upon the rapidity of the expansion.

In addition, the theory does not take into account the difference in time between when the droplets of characteristic size are formed and when the effect can be measured in the main flow. Qualitatively this is well understood. Quantitatively, however, the problem is difficult to evaluate and requires further study.

The general trends qualitatively outlined above are borne out in the present investigations and in those of other authors, as can be seen from an examination of Fig. 1. The Becker-Döring equation, uncorrected for the effect of droplet size on the surface tension of water, is shown for a value of $J = 1$, together with the curve for $J = 1$ when the effect of droplet size on the surface tension (see Fig. 16) has been taken into account.

Previous authors have used for theoretical predictions the uncorrected curve with a value for J of either 1 or 1000, since it is found that either value for J gives almost identical curves. However, such a selection for the value of J has no rational basis whatsoever. The value should be based upon the consideration that a sufficient amount of water vapor has to condense to produce a measurable heating effect. The following considerations show that J should be nearer 10^{16} than 1 or 1000:

The total number of water vapor molecules per cubic centimeter, n_v, is given by

$$n_v = \frac{p_v}{kT} = \frac{\frac{p_v}{p_\infty} \cdot p_\infty}{kT}$$

For example, at a temperature of 233° K. the value for $\ln (p_v/p_\infty)_{th}$ is approximately, from the experimental data with small dynamic effect (Fig. 1):

$$\ln (p_v/p_\infty)_{th} \doteq 2.16$$

or

$$(p_v/p_\infty)_{th} \doteq 8.7 \text{ and } \quad p_\infty = 0.142 \text{ mm. Hg.} = 189 \text{ dynes/cm.}^2$$

Hence,

$$n_v = \frac{8.7\ (189)}{1.381 \times 10^{-16}\ (233)} \doteq 5 \times 10^{16}$$

Furthermore, the number of molecules / cm^3 under saturation conditions at $T = 233°$ K. is

$$n_{v_\infty} = \frac{p_\infty}{kT} \doteq 0.6 \times 10^{16}$$

Thus, the total number of droplets of characteristic size that can be formed per cubic centimeter from the available molecules, whether the

vapor is saturated or unsaturated after the droplets have been formed, is of the order of 4 to 5 x 10^{16} divided by g*, the number of molecules per characteristic droplet.

Fig. 3 shows that, for T = 233° K. and ln (p_v/p_∞) = 2.16, the characteristic droplet presumably has a radius of 4.7 Å and hence, since the radius of a water vapor molecule is about 1.4 Å, contains only 5 to 10 molecules. Therefore, the total number of droplets that can be formed per cubic centimeter, at a temperature of 233° K., is of the order of 10^{16}. Similarly, it can be shown that, over the entire temperature range, this value of 10^{16} remains practically constant.

A completely different approach to the problem is to determine, from an experimental pressure distribution curve, the amount of heat that must have been added to the flow in order to bring about the observed pressure increase through the condensation shock. This value so obtained, together with a knowledge of the time available within the shock for this heat addition process to take place and the size of the characteristic droplet, then determines the necessary nuclei formation frequency.

As an example of this procedure, consider the pressure distribution curve obtained in the Laval nozzle tests, discussed in Part IV, for an initial relative humidity of 32% (see curve 1 of Fig. 6a). The pressure increase across the condensation shock is found to be

$$\frac{p_2}{p_1} = \frac{\frac{p_2}{p_0}}{\frac{p_1}{p_0}} = 1.069$$

Hence, the amount of heat added, q, can be determined from equ. (I.17), Appendix I, since M_1 and a_1 are known. This value is found to be

$$q = 1.13 \text{ gm.cal./gm.}$$

The heat added is related to the number of droplets formed by the equation

$$q = n \cdot (\text{droplet volume}) \cdot L$$

where

n = total number of droplets formed per cm^3.

L = latent heat of vaporization

If it is assumed that all of the droplets formed are of the characteristic size, i.e., the droplet growth across the condensation shock is assumed negligible, then

$$q = n \cdot L \cdot \left(\tfrac{4}{3} \pi r^{*3}\right) \tag{5.1}$$

The nuclei formation frequency, J, is given by the total number of droplets formed per cubic centimeter divided by the time available for this formation, which, in this case, is the time required for the flow to traverse the condensation shock.

Thus,

$$J = n \frac{u}{d} \tag{5.2}$$

where d = thickness of the condensation shock
u = flow velocity

Hence, combining equations (5.2) and 5.1),

$$J = \frac{q u}{L \left(\tfrac{4}{3} \pi r^{*3}\right) \cdot d} \tag{5.3}$$

Using for u a mean value between u_1, which is known, and u_2 which is determined from equ. (I.15) of Appendix I, a value of

4×10^4 cm/sec. is obtained. In addition, the shock thickness, as determined from Fig. 6a, is of the order of 0.3 cm. and r^* is found to be approximately 5×10^{-8} cm (using the known temperature and supersaturation in Fig. 3).

Thus, finally, J is found to be of the order:

$$J = \frac{qu}{L\left(\frac{4}{3}\pi r^{*3}\right)d} \doteq \frac{(1.13)\ (4 \times 10^4)}{677\left[\frac{4}{3}\pi\left(5 \times 10^{-8}\right)^3\right](0.3)} \doteq 4 \times 10^{16}$$

Conversely, if a value for J of 10^3 were to be used, the amount of heat that is added to the flow is determined as

$$q = 3 \times 10^{-22} \text{ gm. cal./gm.}$$

or, the pressure increase due to such an heat addition is approximately:

$$\frac{\Delta p}{p_1} = \frac{p_2 - p_1}{p_1} \doteq 10^{-23}$$

It can be concluded, as a result of the preceding arguments and of the relatively good fit with the experimental data, that the Becker-Döring equation, with a value for J of about 10^{16} and corrected for the effect of droplet size on surface tension, can be used with some assurance to predict the occurrence of condensation in those wind tunnels in which the mixture of water vapor and air is expanded with an axial temperature gradient of about 1° C/cm., or less.

Various values of the mean temperature gradient from the throat to the location of the collapse of the supersaturated state, which essentially determines the rapidity of the expansion, are shown for the different test points in Fig. 1. It is thus seen that, as the temperature gradient increases, the point of collapse

is delayed to higher values of the supersaturation ratio.

A value for J of 10^{24} is shown to correspond fairly closely to the test points obtained from supersonic nozzles with a temperature gradient lying between 15 and 20° C./cm. Such a value for J has no physical significance, however, but is useful for predicting the occurrence of condensation in nozzles with that order of temperature gradient.

PART VI

LOW TEMPERATURE EFFECTS

The observation of Cwilong* that no products of condensation are observed when the final temperature of the humid air, after an adiabatic expansion in a Wilson Cloud Chamber, is below 153° K. (-120° C.), was mentioned briefly in Part I. This observation has such marked implications when considered from the standpoint of condensation in wind tunnels that a series of tests at high Mach numbers was carried out in order to determine whether such a phenomenon existed, or whether it was a peculiarity of the Wilson Cloud Chamber.

With stagnation temperatures of the order of room temperature, air must be expanded to a Mach number of about 2.2 before the local temperature becomes as low as 153° K.. Hence, pressure distribution measurements and Schlieren and light scattering observations were made in the 2.5" x 2.5" Supersonic Wind Tunnel at Mach numbers of 3.0 and 4.0.

In no instance was the condensation observed to start in the test section and travel upstream as the moisture content of the air was increased. This is completely contrary to the observations at the lower Mach numbers, as discussed in Part IV. In all the present tests, as the moisture content was increased to the point where condensation was first observed, the location was found to be only slightly downstream of the throat of the nozzle. Further

---

* loc.cit.

increase in the moisture content then caused the location of the start of condensation to move upstream. The qualitative light scattering observation that no condensation was present before it appeared near the throat was confirmed by the measurement of the static pressure in the test section, which remained constant with increasing moisture content until the aforementioned point was reached, whereupon it started increasing.

Furthermore, for a small range of initial relative humidities beyond that at which the condensation first became visible, no condensation could be observed in the test section. It is not to be concluded from this observation that the droplets vaporized again, although such could be the case, since the area of the test section is much greater than that at the point where the condensation occurred and hence the droplet concentration could become so low as to exhibit negligible light scattering. It does, however, indicate that the droplets do not increase appreciably in either size or number downstream of the start of condensation, over this particular range of initial relative humidities. As the initial relative humidity is increased further, the condensation becomes, at first, faintly visible in the test section and then gradually increases.

The static pressure in the test section in the form p/p_o, is shown in Fig. 8 as a function of the initial relative humidity, together with the corresponding qualitative observations of the light scattering technique.

These investigations show that, for Mach numbers such that the

local temperature is below 153° K., test section pressure measurements alone would determine a particular value of the initial relative humidity at which condensation first occurred at that Mach number; whereas, in reality, the condensation is not occurring in the test section, but far upstream.

Of far more importance is the phenomenon itself. No definite explanation can be given at the present time for this, apparently, anomalous behaviour. If the phenomenon does exist, as these investigations indicate, it is to be expected that if the flow is expanded from the throat sufficiently fast, so that condensation does not have time to occur before a temperature of 153° K. is reached, then no condensation will take place at all. This latter conclusion appears to be borne out by some preliminary observations in the GALCIT Hypersonic Wind Tunnel at a Mach number of 6, since no condensation has been observed even though the dew point has been about 60° F. The densities in the test section are so low at these Mach numbers, however, that these observations cannot be considered conclusive.

PART VII

THE EFFECT OF THE PRESENCE OF DROPLETS IN SUPERSONIC WIND TUNNEL TESTS.

In addition to the effect of the heat addition resulting from the collapse of the supersaturated state, the presence of droplets in the flow can have an effect on the results obtained from supersonic wind tunnel tests. Several of these effects are discussed briefly below.

A. The Increase in the Coefficient of Viscosity.

If the droplets present in the air are assumed to be rigid spheres and if the total volume of the droplets in a unit volume of the mixture is small compared with the unit volume, Einstein[30] has shown that the viscosity of air containing droplets is greater than that of air alone by the factor

$$\frac{\mu'}{\mu} = 1 + 2.5\,\Omega$$

where μ' = viscosity of air containing droplets

μ = viscosity of air alone

Ω = total volume of the droplets/unit volume

But, $\Omega = \left(\Sigma N_r \cdot \frac{4}{3}\pi r^3 \right) / \text{cm.}^3$, and hence in order to determine the viscosity in, e.g., the test section, the mass rate of condensation must be integrated along the nozzle from the point where droplets first form to the test section. However, an approximate upper bound for this effect can be determined easily in the following manner:

Consider water vapor in air at a temperature of 0° C. and at the threshold supersaturation ratio corresponding to that temperature,

i.e., $\ln p_v/p_\infty \doteq 2.5$ or $p_v/p_\infty \doteq 12.2$. The total number of water molecules at that point is then

$$n_v = \frac{p/p_\infty \cdot p_\infty}{kT} \doteq \frac{12.2\,(6.1\times10^{3})}{1.381\times10^{-16}\,(273)} \doteq 2\times10^{18} \text{ MOLECULES/CM.}^3$$

If it is assumed that all of these molecules condense into N_r droplets of radius r, then

$$N_r \cdot \frac{4}{3}\pi r^3 \cdot \frac{\rho N_o}{m} = n_v$$

or,

$$\Omega = N_r \cdot \frac{4}{3}\pi r^3 = n_v \cdot \frac{m}{\rho N_o} \doteq 2\times10^{18}\left(3\times10^{-23}\right) \doteq 6\times10^{-5}$$

Hence,

$$\frac{\mu'}{\mu} \doteq 1 + 1.5 \times 10^{-4}$$

Thus it is seen that the effect of the droplets on the viscosity of the air is negligible under normal conditions.

B. THE CHANGE IN THE STRENGTH OF SHOCK WAVES.

The strength of a shock wave existing in supersonic flow that is free of condensation, e.g. the shock wave from the leading edge of a wing, is affected by the presence of droplets in the flow, even for the same free stream conditions ahead of the shock. This effect arises because the change in the flow parameters across the shock, i.e.,the increase in temperature and pressure and the decrease in Mach number, is such as to cause an evaporation of the droplets. From Appendix I, it is seen that for this case, which corresponds to the normal shock with negative heat addition, the pressure and density increase across the shock is always greater and the entropy increase always less than that across a normal shock in the absence of droplets. A comparison of the Schlieren pictures of Fig. 11 e) and f),

showing the shock waves over an airfoil in transonic flow, with and without droplets present in the flow, bears out this difference in the density increase.

Furthermore, for an oblique shock wave emanating from, say, the leading edge of a double-wedge airfoil, since the flow deflection angle must be the same whether or not there are droplets in the flow, it can be shown as follows that the oblique shock with vaporization must be more inclined into the direction of the flow than the oblique shock without vaporization, for the same free stream conditions ahead of the shock:

Let u be the component of the velocity, w, normal to and v the component parallel to the oblique shock wave, which is at an angle β to the free stream direction. For the same free stream temperature and Mach number, M_o, and same flow deflection angle δ, e.g. considering a wedge of half-angle δ under given free stream conditions, the following relations are obtained from the geometry of the flow:

$$\frac{u_2}{u_1} = \frac{w_2 \sin(\beta-\delta)}{w_1 \sin\beta} = \frac{v_2}{v_1}\,\frac{\cos\beta}{\cos(\beta-\delta)} \cdot \frac{\sin(\beta-\delta)}{\sin\beta} = \frac{\tan(\beta-\delta)}{\tan\beta}$$

since $v_2 = v_1$ from the continuity equation.

Similarly,

$$\frac{u_2'}{u_1'} = \frac{\tan(\beta'-\delta)}{\tan\beta'}$$

where the subscripts 1 and 2 denote conditions ahead of and behind the oblique shock, resp., and the prime refers to the oblique shock

with vaporization.

Thus,

$$\frac{\frac{u_2'}{u_1'}}{\frac{u_2}{u_1}} = \frac{TAN(\beta' - \delta)}{TAN(\beta - \delta)} \cdot \frac{TAN\,\beta}{TAN\,\beta'} \qquad (7.1)$$

for the same flow deflection angle.

From equation (I.15), Appendix I,

$$\frac{u_2'}{u_1'} = \frac{1}{(\gamma+1)M_1'^2}\left[(1+\gamma M_1'^2) - (M_1'^2-1)\sqrt{1 - \frac{2(\gamma^2-1)M_1'^2}{a_1^2(M_1'^2-1)^2}\cdot q}\right] \qquad (I.15a)$$

where q is now negative, corresponding to vaporization within the shock. If an amount of vaporization is obtained such that $(-q) = (-q^*) = \left[-\frac{a_1^2(M_1'^2-1)^2}{2(\gamma^2-1)M_1'^2}\right]$, equation (I.15a) reduces to

$$\frac{u_2'}{u_1'} = \frac{(\gamma - \sqrt{2})M_1'^2 + (1+\sqrt{2})}{(\gamma+1)M_1'^2}$$

If, however, for purposes of computation, an amount of vaporization slightly less than this value is considered, such that $(-q) = 0.96\,(-q^*)$, then equation (I.15a) becomes

$$\frac{u_2'}{u_1'} = \frac{(\gamma - \sqrt{\gamma^2})M_1'^2 + (1+\sqrt{\gamma^2})}{(\gamma+1)M_1'^2} = \frac{1}{M_1'^2}$$

For the oblique shock with no vaporization ($q = 0$), equation (I.15a) takes the form

$$\frac{u_2}{u_1} = \frac{(\gamma-1)M_1^2 + 2}{(\gamma+1)M_1^2}$$

Whence,

$$\frac{\frac{u_2'}{u_1'}}{\frac{u_2}{u_1}} = \frac{M_1'^2}{M_1'^2}\cdot\frac{\gamma+1}{(\gamma-1)M_1^2+2} = \frac{SIN^2\beta}{SIN^2\beta'}\cdot\frac{\gamma+1}{(\gamma-1)M_1^2+2} \qquad (7.2)$$

since, for $M_o = M_o'$,

$$\frac{M_1^2}{M_1'^2} = \frac{M_o^2 \sin^2\beta}{M_o^2 \sin^2\beta'} = \frac{\sin^2\beta}{\sin^2\beta'}$$

Combining equations (7.1) and (7.2),

$$\frac{\tan(\beta'-\delta)}{\tan(\beta-\delta)} \cdot \frac{\tan\beta}{\tan\beta'} \cdot \frac{\sin^2\beta'}{\sin^2\beta} = \frac{1}{\frac{\gamma-1}{\gamma+1} M_1^2 + \frac{2}{\gamma+1}}$$

or,

$$\tan(\beta'-\delta)\sin 2\beta' = \frac{\tan(\beta-\delta)\sin 2\beta}{\frac{\gamma-1}{\gamma+1} M_o^2 \sin^2\beta + \frac{2}{\gamma+1}} \qquad (7.3)$$

Equation (7.3) is plotted in Fig. 10 in the form of the free stream Mach number as obtained from the oblique shock chart using the shock angle measured from, say, a Schlieren photograph vs. the true free stream Mach number for several values of wedge half-angle, when an amount of vaporization given by $(-q) = 0.96\ (-q^*)$ takes place across the oblique shock. From this figure it is seen that the error in Mach number can vary from zero per cent, for no droplets in the flow, up to several hundred per cent for a large half-angle wedge at high Mach number, with this particular amount of vaporization.

This analysis shows that, unless the amount of vaporization in each case is known, the utilization of the oblique shock angle to determine the free stream Mach number is highly questionable.

C. THE EFFECT OF DROPLETS ON WIND TUNNEL MODELS

The trajectories of small water droplets in air moving at high velocities around a cylinder have been calculated by Langmuir and Blodgett (31). They find that the trajectories depend upon

the dimensionless quantity

$$2\rho_\ell r^2 \frac{w}{9} \mu R$$

where R is the radius of the cylinder. It is shown that when the droplets are so small that this quantity becomes less than 1/8, no deposition occurs on any part of the cylinder. Thus, for a flow velocity of 400 m./sec. around a cylinder of 1 mm radius, it is seen that the droplets first formed, which are less than 10^{-7} cm., will not be deposited upon the cylinder and that it is not until the droplets grow to a size of about 10^{-5} cm. that deposition will occur. As a result, it is to be expected that impingement of droplets on wind tunnel models will only occur in those cases where the condensation has taken place a considerable distance upstream of the model and where, in addition, the expansion takes place at a slow enough rate to enable the droplets to attain a size of about 10^{-5} cm. or larger. A rapid expansion tends to retard the rate of droplet growth because, whereas continued expansion following the condensation favors the growth of the droplets, a rapid expansion results in a greater temperature difference between that of the droplet and that of the surrounding air, since the droplets have a higher heat capacity and hence will lag behind the decreasing temperature of the air.

These considerations have been demonstrated in all of the 2.5" Supersonic Wind Tunnel tests performed in this investigation, where

although the condensation occurred as far upstream of the model as 20 diameters, no deposition of droplets on the model occurred because of the rapid expansion rate. No deposition would be expected if the condensation were in the form of ice particles rather than liquid droplets; however in these instances the temperatures were such that supercooled water was still predominant.

In those cases where large droplets have been attained, the effect of their impact upon the model can be considerable. The actual impulse of such impacts will normally be negligible, but the freezing of the supercooled droplets on the model will, of course, markedly affect the flow.

The effect of the presence of droplets in the boundary layer has not been investigated, but a few qualitative remarks can be made. It is shown in Appendix I that flow with vaporization results in a decrease in Mach number if the flow is subsonic and an increase if it is supersonic. Hence, the Mach number in the subsonic and supersonic portions of the boundary layer will be correspondingly affected by the vaporization of droplets. Furthermore, the vaporization of droplets within the boundary layer should result in a decrease in the temperature gradient in the outer part of the boundary layer, where heat is being absorbed in the vaporization process, and hence a large temperature gradient immediately next to the wall.

The effect of these factors on the frictional drag of a body or on transition has not been investigated, but bears further study.

PART VIII

THE POSSIBLE INFLUENCE OF TURBULENCE

Although no systematic investigation of the effect of turbulence on spontaneous condensation was undertaken, a few qualitative remarks can be made.

Turbulence may promote an earlier collapse of the supersaturated state and a more rapid growth of the droplets by a) maintaining a given supersaturated state for a longer time than is the case in the absence of turbulence and thus decreasing the dynamic effect and b) causing locally higher supersaturations through the change in the flow parameters in turbulent eddies.

These statements are believed to be vividly demonstrated by Figures 11a and 11c. In these instances, a 12% thick, bi-convex airfoil was mounted between the Schlieren windows in the 2" x 20" Transonic Wind Tunnel, which was operated in the free stream Mach number range of 0.78 to 0.91. At a fixed Mach number, the stagnation temperature was gradually decreased until condensation could be observed by means of the light scattering technique. This first appearance of condensation manifested itself in the form of two distinct sheets of condensation which were approximately symmetrical about the centerline of the tunnel and varying distances apart depending upon the free stream Mach number. The condensation sheets started downstream of the shock wave that occurred over the airfoil, as observed with the Schlieren system, with no other condensation detectable in the wind tunnel. As the stagnation

temperature was decreased still further, condensation was visible throughout the whole test section, but the condensation sheets were readily apparent because of the much greater intensity of the condensation in that region.

In order to determine the effect of the type of shock wave, i.e., a laminar-boundary-layer or turbulent-boundary-layer-type (to be called a laminar-type and turbulent-type hereafter, for brevity), on the condensation sheets, a wire of 0.024 inch diameter was located parallel to the leading edge of the airfoil, approximately on the centerline of the wind tunnel and just upstream of the Schlieren windows. This arrangement produced a turbulent-type of shock wave over the airfoil, in contrast to the laminar-type in the absence of the wire. It is seen in the photographs that the wire, also, produced two condensation sheets that flowed around the airfoil and then remained a small distance apart. Thus, for a comparison between the effects of the two types of shock waves, only the higher Mach number tests can be used, where the condensation sheets from the turbulent-type of shock wave are distinct from those of the wire.

From Figures 11a and 11c, which show the condensation sheets from the laminar-type and the turbulent-type of shock wave, resp., it is seen that, at the same free stream Mach number, the condensation sheets from the two types are about the same distance apart. The only marked difference between the two is the thickness and intensity of the scattered light of the individual condensation sheets, which is greater for the laminar-type, and the distance

downstream of the shock wave at which they start, which is greater for the turbulent-type. Thus, the condensation sheets are more intense and start earlier in the case of the laminar-type shock wave than in the turbulent-type. If, as is believed to be the case, a vortex sheet is produced downstream of the intersection of the oblique shock with the normal, in the laminar-type shock, and downstream of the region where the turbulent-type of shock wave suddenly changes curvature, it is to be expected that the vortex sheet downstream of the laminar-type would be the more intense. The difference in intensities of the condensation sheets bears out such an explanation.

Attributing the phenomenon of these condensation sheets to the effects of turbulence, is, at the present time, pure conjecture. However, their appearance prior to that of any other condensation in the flow, together with their high intensity, make such an explanation plausible.

APPENDIX I

SHOCK RELATIONS FOR FLOW WITH CONDENSATION

If it is assumed that no condensation takes place prior to the threshold supersaturation ratio and that the supersaturated state collapses completely when the latter point is reached, the change in the flow parameters as a result of the condensation can be determined by considering the normal shock relations with heat addition. This problem has been treated by numerous investigators, e.g., Samaras [32], Heybey [33], and Charyk*, as has the analogous problem of compressible flow with continuous heat addition, which has been worked out by Hicks, et al [34], and others.

The development of the one-dimensional shock relations with heat addition is included herein in order that an extension to the case where the heat addition is small can be made and thence be compared with the normal shock relations with no addition of heat. Furthermore, since only one of the two possible solutions of the equations has been discussed in the literature, it is desired to consider the other possible solution in more detail.

It is assumed in the following analysis that the provisions exist for the necessary heat and mass transfer upon condensation, i.e., that the problem can be considered as an instantaneous heat addition process, and that the energy of the liquid phase that exists downstream of the condensation region has a negligible effect on the energy equation.

Using subscripts 1 and 2 to denote conditions upstream and downstream of the discontinuity, resp., and employing standard notation

---

* loc. cit.

(see, e.g., Liepmann and Puckett [35], p. 38) except where noted, the equations of continuity, momentum and energy across a discontinuity with heat addition become:

$$\rho_1 u_1 = \rho_2 u_2 \qquad \text{Equation of Continuity} \qquad (I.1)$$

$$p_2 - p_1 = \rho_1 u_1^2 - \rho_2 u_2^2 \qquad \text{Conservation of Momentum} \qquad (I.2)$$

or

$$\left.\begin{aligned} &\frac{1}{2} u_1^2 + \frac{a_1^2}{\gamma-1} + q = \frac{1}{2} u_2^2 + \frac{a_2^2}{\gamma-1} \\ &\frac{\gamma+1}{2(\gamma-1)} a_1^{*2} + q = \frac{\gamma+1}{2(\gamma-1)} a_2^{*2} \end{aligned}\right\} \qquad \text{Conservation of Energy} \qquad (I.3)$$

where q is the total amount of heat added as a result of the condensation. The change in γ across the discontinuity is assumed negligible.

From equations (I.1), (I.2) and the relation, $a^2 = \gamma \frac{p}{\rho}$

$$\frac{p_2}{\rho_2 u_2} - \frac{p_1}{\rho_1 u_1} = u_1 - u_2 = \frac{1}{\gamma}\left[\frac{a_2^2}{u_2} - \frac{a_1^2}{u_1}\right] \qquad (I.4)$$

From equations (I.3), letting $a_1^{*2} \equiv a^{*2}$

$$a_2^2 = \frac{\gamma+1}{2} a^{*2} + (\gamma-1) q - \frac{\gamma-1}{2} u_2^2$$

and

$$a_1^2 = \frac{\gamma+1}{2} a^{*2} - \frac{\gamma-1}{2} u_1^2$$

Introducing these equations into equation (I.4), the following equation for u_2 is obtained

$$u_2^2 - \frac{u_1^2 + a^{*2}}{u_1} u_2 + \left(a^{*2} + 2\frac{\gamma-1}{\gamma+1} q\right) = 0$$

Whence,

$$u_2 = \frac{u_1^2 + a^{*2}}{2u_1}\left[1 \pm \sqrt{1 - \frac{4\left(a^{*2} + 2\frac{\gamma-1}{\gamma+1} q\right) u_1^2}{(u_1^2 + a^{*2})^2}}\right]$$

or, in a slightly different form,

$$u_1 u_2 = \frac{1}{2}\left[(u_1^2+a^{*2}) \pm (u_1^2-a^{*2})\sqrt{1-\frac{8\frac{\gamma-1}{\gamma+1}u_1^2 q}{(u_1^2-a^{*2})^2}}\right] \qquad (I.5)$$

Thus, there are two possible solutions, where i) the minus sign denotes a shock with condensation and ii) the plus sign denotes a condensation shock. For example, for q = 0, equation (I.5) becomes

i) $u_1 u_2 = a^{*2}$ which is the solution for a normal shock

and ii) $u_1 u_2 = u_1^2$, i.e., $u_1 = u_2$

If q is small, such that the right hand term under the square root is small compared with unity, equation (I.5) becomes

$$u_1 u_2 \doteq \frac{1}{2}\left[(u_1^2+a^{*2}) \pm (u_1^2-a^{*2}) \mp \frac{4\frac{\gamma-1}{\gamma+1}u_1^2}{u_1^2-a^{*2}} q\right] \qquad (I.6)$$

Consider first the normal shock with weak condensation, case (i). Equation (I.6) becomes

$$u_1 u_2 \doteq a^{*2} + \frac{2\frac{\gamma-1}{\gamma+1}u_1^2}{u_1^2-a^{*2}} q \qquad (I.7)$$

From equations (I.1) and (I.2), the pressure change across the shock can be expressed as

$$\frac{p_2-p_1}{p_1} = \frac{\rho_1}{p_1}(u_1^2 - u_1 u_2) \doteq \frac{\gamma}{a_1^2}\left[(u_1^2-a^{*2}) - \frac{2\frac{\gamma-1}{\gamma+1}u_1^2}{u_1^2-a^{*2}} q\right]$$

or, since $(u_1^2 - a^{*2}) = \frac{2}{\gamma+1}(u_1^2 - a_1^2)$, in terms of the Mach number in front of the shock, this equation becomes

$$\frac{p_2-p_1}{p_1} = \frac{2\gamma}{\gamma+1}(M_1^2-1)\left[1 - \frac{\gamma^2-1}{2}\cdot\frac{M_1^2}{(M_1^2-1)^2 a_1^2} q\right] \qquad (I.8)$$

The multiplying factor in equation (I.8) is the pressure increase

across a normal shock without condensation. Hence, the pressure increase in the normal shock with condensation is always less than the pressure increase without condensation.

Similarly, the density increase is determined as

$$\frac{\rho_2}{\rho_1} = \frac{(\gamma+1)M_1^2}{(\gamma+1)M_1^2+2}\left[1 - \frac{(\gamma^2-1)M_1^2}{(M_1^2-1)\,a_1^2\left[(\gamma-1)M_1^2+2\right]}\,q\right] \qquad (I.9)$$

and hence the same remarks apply as for the pressure increase.

The change in entropy across a normal shock with condensation is of interest and is determined from the relation

$$\frac{\Delta S}{C_v} = \log\left(\frac{p_2}{p_1}\right)\left(\frac{\rho_1}{\rho_2}\right)^{\gamma}$$

and equations (I.8) and (I.9). For M_1 near unity, if

$$M_1^2 = 1 + m \quad \text{and} \quad m << 1$$

the change in entropy becomes

$$\frac{\Delta S}{C_v} = \log\left[1 + \frac{2\gamma}{\gamma+1}\,m - \frac{\gamma(\gamma-1)(1+m)}{a_1^2\,m}\,q\right]\cdot\left[1 + \frac{\gamma-1}{\gamma+1}\,m + \frac{(\gamma-1)(1+m)}{a_1^2\,m}\,q\right]^{\gamma}\cdot(1+m)^{-\gamma}$$

Expanding this in a power series in m and q, using the expansion for $\log(1+x)$, and neglecting the higher order terms, it is found that

$$\frac{\Delta S}{C_v} = \frac{\gamma(\gamma-1)(1+m)\,q}{a_1^2} + \frac{2}{3}\,\frac{\gamma(\gamma-1)\,m^3}{(\gamma+1)^2} + \cdots$$

or

$$\frac{\Delta S}{R} = \frac{\gamma M_1^2}{a_1^2}\,q + \frac{2\gamma}{(\gamma+1)^2}\,\frac{(M_1^2-1)^3}{3} \qquad (I.10)$$

Since the second term on the right hand side of equation (I.10) is

the first term in the expansion for a normal shock without condensation, it is seen that the entropy increase is greater through a normal shock with condensation.

Furthermore, considering only these lowest order terms, it is apparent that if $q > \frac{2a_1^2(M_1^2-1)^3}{3(\gamma+1)^2 M_1^2}$ when $M_1 < 1$, then a normal shock with condensation could exist in subsonic flow, provided a positive change in entropy is the only criterion.

Consider now the weak condensation shock, case (ii). Equation (I.6) then becomes

$$u_1 u_2 = u_1^2 - \frac{2\frac{\gamma-1}{\gamma+1}u_1^2 q}{u_1^2 - a^{*2}} = u_1^2 - \frac{(\gamma-1)M_1^2}{(M_1^2-1)}q$$

Whence, the following relations are derived in a manner similar to that in case (i):

$$\frac{p_2}{p_1} = 1 + \frac{\gamma(\gamma-1)M_1^2}{a_1^2(M_1^2-1)}q \qquad \text{(I.11)}$$

$$\frac{\rho_2}{\rho_1} = 1 + \frac{\gamma-1}{a_1^2(M_1^2-1)}q \qquad \text{(I.12)}$$

$$\frac{M_2}{M_1} = 1 - \frac{\gamma-1}{2}\cdot\frac{(\gamma M_1^2+1)}{a_1^2(M_1^2-1)}q \qquad \text{(I.13)}$$

$$\frac{T_2}{T_1} = 1 + \frac{(\gamma-1)(\gamma M_1^2-1)}{a_1^2(M_1^2-1)}\cdot q \qquad \text{(I.14)}$$

$\frac{\Delta S}{R} = \frac{\gamma}{a_1^2}\cdot q$ for a weak condensation shock near $M_1 = 1$ (i.e., $M_1 = 1 \pm m$).

From equations (I.11) through (I.14), the following conclusions can be drawn as regards the change in the flow parameters across a condensation shock:

a) $\frac{p_2}{p_1}\begin{cases} <1 & \text{FOR } M_1 < 1 \\ >1 & \text{FOR } M_1 > 1 \end{cases}$

b) $\frac{\rho_2}{\rho_1}\begin{cases} <1 & \text{FOR } M_1 < 1 \\ >1 & \text{FOR } M_1 > 1 \end{cases}$

c) $\frac{M_2}{M_1}\begin{cases} >1 & \text{FOR } M_1 < 1 \\ <1 & \text{FOR } M_1 > 1 \end{cases}$

d) $\frac{T_2}{T_1}\begin{cases} >1 & \text{FOR } 0 \le M_1 < \frac{1}{\sqrt{\gamma}} = 0.845 \\ <1 & \text{FOR } 0.845 < M_1 < 1 \\ >1 & \text{FOR } M_1 > 1 \end{cases}$

Thus, one of the usual conclusions is reached, that the Mach number behind a condensation shock decreases toward unity if the initial flow is supersonic and increases toward unity if the initial flow is subsonic. Hence, a supersonic flow cannot become a subsonic by means of a condensation shock alone.

If equation (I.5) be written in terms of the initial Mach number, M_1, i.e.

$$u_1 u_2 = \frac{a_1^2}{\gamma+1}\left[(1+\gamma M_1^2) \pm (M_1^2-1)\sqrt{1-\frac{2(\gamma^2-1)M_1^2}{a_1^2(M_1^2-1)^2}\cdot q}\right] \qquad \text{(I.15)}$$

it is seen that the maximum amount of heat that can be added to the flow is

$$q_{MAX} = \frac{a_1^2(M_1^2-1)^2}{2(\gamma^2-1)M_1^2} \qquad \text{(I.16)}$$

Considering the general "exact" equation for the pressure change across either a normal shock with condensation or a condensation shock,

$$\frac{P_2 - P_1}{P_1} = \frac{\gamma}{\gamma+1}\left(M_1^2 - 1\right)\left\{1 \mp \sqrt{1 - \frac{2\left(\gamma^2-1\right)M_1^2}{a_1^2\left(M_1^2-1\right)^2}\cdot q}\right\} \qquad (I.17)$$

it is to be noted that, with the maximum addition of heat, the pressure change is the same across both types of discontinuities and is equal to one-half that across a normal shock without condensation. Furthermore, the intensity of the normal shock with condensation is a maximum when $q = 0$, whereas the intensity of a condensation shock is a maximum when $q = q_{max}$.

Similarly, it can be shown that, with the maximum addition of heat, the Mach number is always unity downstream of either type of discontinuity, regardless of the initial Mach number of the flow. Also, for an addition of heat less than the maximum, the Mach number downstream of a normal shock with condensation is greater than unity if the flow is initially subsonic and less than unity if it is initially supersonic.

From these observations on the change in pressure and Mach number across the two possible types of discontinuities, it can be concluded that the shock observed at the location where the condensation commences in a supersonic nozzle is a condensation shock, since a) the intensity of the shock decreases as the air is dried and b) the Mach number downstream of the shock is still supersonic.

However, there may be instances in which the normal shock with condensation does occur, since, unless considerations other than that of the change in entropy prove otherwise, such a discontinuity can exist. Furthermore, the normal shock with vaporization, which was discussed in Part VII-B, represents just such a case.

APPENDIX II

COMPUTATIONAL PROCEDURES

Inasmuch as the prime interest in spontaneous condensation as applied to supersonic wind tunnels is in how to avoid it, a few typical examples with this end in mind will be calulated.

1. Suppose that it is desired to determine how high the stagnation temperature must be raised in order to avoid the condensation of the water vapor in air that has a stagnation dew point* of 68° F., when it is to be expanded fairly rapidly, i.e. $\Delta T/\Delta x \simeq 15°C./cm.$, to a Mach number of 1.4. (The stagnation pressure is assumed to be 760 mm. Hg.):

a) From Fig. 13, the partial pressure of the water vapor, p_{v_o}, corresponding to a stagnation dew point temperature of 68° F. (293° K.) is found to be 17.5 mm. Hg..

b) The mixing ratio, χ, is determined from equ. (2.6) or Fig. 14 as 0.00147. Hence, Fig. 12 shows that the presence of the water vapor in the air can be neglected during the isentropic expansion (see Appendix III).

c) Isentropic tables or charts are used to determine the pressure and temperature ratios corresponding to a Mach number of 1.4. Thus, $p/p_o = 0.3142$ and $T/T_o = 0.7184$. Moreover, from equ. (2.7), $P_v/p_{v_o} = p/p_o = 0.3142$.

d) The supersaturation ratio, p_v/p_∞, is determined from the relation

$$\frac{P_v}{p_\infty} = \frac{P_v}{P_{v_o}} \cdot \frac{P_{v_o}}{p_\infty} = \frac{5.50}{p_\infty}$$

---

* It should be pointed out that if the dew point is not measured at stagnation pressure, but at some other pressure p_d, then the partial pressure of the water vapor at stagnation conditions is obtained from the relation $p_{v_o} = p_{v_d} \times \frac{p_o}{p_d}$

where p_v/p_∞ is the threshold value as determined from Fig. 1, for $\Delta T/\Delta x \simeq 15^\circ C./cm$ ($J = 10^{24}$), corresponding to the temperature at a Mach number of 1.4 and p_∞ is the saturation vapor pressure corresponding to that temperature. Hence, a trial-and-error procedure must be used to find the temperature for which the above equality holds. This is found to be 235.6° K.

e) The minimum required stagnation temperature is then obtained from the isentropic relation. This is: $T = 328^\circ$ K. = 131° F. (It should be noted, however, that unless the flow is expanded rapidly, i.e. greater than $1^\circ C./cm$, from that point in the nozzle where a Mach number of 1.15 is attained onward, condensation will occur just downstream of the throat. This problem will be treated more fully in the next example.)

2. Suppose that the stagnation temperature of a supersonic wind tunnel is 77° F. (298° K.) and the stagnation dew point is 14° F. (265° K.). It is desired to determine the Mach number to which the air can be expanded before condensation takes place:

This problem is solved most easily by determining the supersaturation ratio at various stations along the nozzle in the following manner:

a) Arbitrarily select various values for the Mach number and therefrom determine the temperature and the pressure ratio from the isentropic relations.

b) The saturation vapor pressure corresponding to the above temperatures is obtained from Fig. 13.

c) The supersaturation ratio corresponding to these temperatures is then determined as in (d) above, since p_{v_o} is known.

d) The natural logarithm of the supersaturation ratio is plotted against the temperature.

This procedure has been carried out for a stagnation temperature of 298° K. and a stagnation dew point of 263° K. and the result presented as curve A-B in Fig. 1.

It is seen from Fig. 1 that condensation will not occur near the throat, where there is normally a negligible dynamic effect, if the expansion is rapid enough such that a temperature gradient greater than 1°C./cm. is attained by the time the flow reaches a Mach number of 1.2 ($T = 231.4^\circ$ K. and $\ln (P_v/P_\infty) = 1.98$). Thus, if the temperature gradient is of the order of 15°C./cm., condensation will occur at a Mach number slightly higher than 1.60 ($T = 197.1^\circ$ K. and $\ln (P_v/P_\infty) = 5.70$)

If, however, an increasingly greater temperature gradient is maintained, such that condensation does not occur until a Mach number of about 2.1 (corresponding to a temperature of about 153° K.) is reached, then condensation should not occur, regardless of how highly supersaturated the vapor becomes or of how rapidly the expansion is carried out beyond that point.

APPENDIX III

ERRORS INVOLVED IN NEGLECTING THE PRESENCE OF WATER VAPOR IN THE ISENTROPIC EXPANSION OF HUMID AIR.

Practically all existing gas dynamics tables are based upon the constants for dry air, which assumes that the effect of any water vapor present in the air is negligible. The validity of this assumption can be checked in the following manner:

For the isentropic flow of dry air in a supersonic nozzle, the area-ratio is related to the Mach number by the equation (see Liepmann and Puckett*, p. 34)

$$\left(\frac{A}{A^*}\right)_a^2 = \frac{1}{M_a}\left[\frac{2}{\gamma+1}\left(1+\frac{\gamma-1}{2}M_a^2\right)\right]^{\frac{\gamma+1}{\gamma-1}} \qquad \text{(III.1)}$$

or, in terms of the temperature ratio, $T_o/T = 1 + \frac{\gamma-1}{2}M^2$,

$$\left(\frac{A}{A^*}\right)_a^2 = \frac{\frac{\gamma-1}{2}}{\left(\frac{T_o}{T}\right)_a - 1}\left[\frac{2}{\gamma+1}\left(\frac{T_o}{T}\right)_a\right]^{\frac{\gamma+1}{\gamma-1}} \qquad \text{(III.2)}$$

Similarly, the area-ratio for the isentropic flow of humid air, designated by subscript m, is given by

$$\left(\frac{A}{A^*}\right)_m^2 = \frac{\frac{\gamma'-1}{2}}{\left(\frac{T_o}{T}\right)_m - 1}\left[\frac{2}{\gamma'+1}\left(\frac{T_o}{T}\right)_m\right]^{\frac{\gamma'+1}{\gamma'-1}} \qquad \text{(III.3)}$$

where, γ' is the ratio of the specific heats for the humid air.

Hence, at the same location in the nozzle (i.e., $(A/A^*)_a = (A/A^*)_m$), the relation between the two temperature ratios is given by

$$\frac{\frac{\gamma-1}{2}}{\left(\frac{T_o}{T}\right)_a - 1}\left[\frac{2}{\gamma+1}\left(\frac{T_o}{T}\right)_a\right]^{\frac{\gamma+1}{\gamma-1}} = \frac{\frac{\gamma'-1}{2}}{\left(\frac{T_o}{T}\right)_m - 1}\left[\frac{2}{\gamma'+1}\left(\frac{T_o}{T}\right)_m\right]^{\frac{\gamma'+1}{\gamma'-1}}$$

* loc. cit.

or,

$$\frac{\left[\frac{2}{\gamma+1}\left(\frac{T_o}{T}\right)_a\right]^{\frac{\gamma+1}{\gamma-1}}}{\left[\frac{2}{\gamma'+1}\left(\frac{T_o}{T}\right)_m\right]^{\frac{\gamma'+1}{\gamma'-1}}} = \frac{\gamma'-1}{\gamma-1}\,\frac{\left(\frac{T_o}{T}\right)_a - 1}{\left(\frac{T_o}{T}\right)_m - 1} \tag{III.4}$$

This equation can be written in the form

$$\left(\frac{T}{T_o}\right)_a = (1-\varepsilon_T)\left(\frac{T}{T_o}\right)_m \tag{III.5}$$

where ε_T is a correction term that depends upon the amount of water vapor in the air, the latter being given by the mixing ratio, x.

The relationship between the pressure ratios, $(p/p_o)_a$ and $(p/p_o)_m$, is obtained as follows:

$$\left(\frac{T}{T_o}\right)_a = \left(\frac{P}{P_o}\right)_a^{\frac{\gamma-1}{\gamma}} \quad \text{and} \quad \left(\frac{T}{T_o}\right)_m = \left(\frac{P}{P_o}\right)_m^{\frac{\gamma'-1}{\gamma'}} \tag{III.6}$$

But, from equation (2.8),

$$\frac{\gamma'-1}{\gamma'} = \frac{R\left(\frac{1}{m_a}+\frac{\chi}{m_v}\right)}{c_{p_a}+\chi c_{p_v}} = \frac{\gamma-1}{\gamma}\cdot\left[\frac{1+\frac{\chi}{\varepsilon}}{1+\chi\cdot\frac{c_{p_v}}{c_{p_a}}}\right] = \frac{\gamma-1}{\gamma}\cdot\alpha$$

Hence, utilizing this relationship together with equation (III.5), equation (III.6) becomes

$$\left(\frac{P}{P_o}\right)_a^{\frac{\gamma-1}{\gamma}} = (1-\varepsilon_T)\left(\frac{P}{P_o}\right)_m^{\frac{\gamma-1}{\gamma}\cdot\alpha}$$

or,

$$\left(\frac{P}{P_o}\right)_a = (1-\varepsilon_p)\left(\frac{P}{P_o}\right)_m^{\alpha} = (1-\varepsilon_p)\left(\frac{P}{P_o}\right)_m^{1-\varepsilon'_p} \tag{III.7}$$

The relationship between the Mach numbers is given by

or

$$M_a = (1 + \varepsilon_m)\, M_m \qquad \text{(III.8)}$$

The correction factors, ε_T, ε_p, ε_p' and ε_M, for use in equations (III.5), (III.7) and (III.8) are plotted in Fig. 12 as a function of the mixing ratio.

An examination of this figure shows that the error in p/p_o is given fairly accurately by the actual value of the mixing ratio. For example, in the Laval nozzle pressure distribution measurements discussed in Section IV B, where the mixing ratio was 0.003 gms. of water vapor / gm. of dry air, the error in assuming that the pressure ratio is that corresponding to dry air is only 0.3%, which is of the order of the accuracy of the original measurements.

APPENDIX IV

ADDITIONAL EXPERIMENTAL TECHNIQUES

Several additional techniques, not described in Section III, that were tried during the course of this investigation (with the exception of "A") are of value in certain instances and hence are discussed briefly.

A. Stagnation Temperature Measurements

A stagnation temperature probe could be used to determine the intensity of collapse, inasmuch as it has an advantage over the total pressure probe in that the only change in stagnation temperature is that connected with the addition of heat due to the condensation. However, a brief calculation will show that the stagnation temperature is much less sensitive than the stagnation pressure to changes in the heat added to the flow, which, coupled with the problems involved in shielding the thermocouple, etc., make this technique undesirable.

B. Diffraction Rings

When a medium containing finely dispersed particles is interposed between a monochromatic point source of light and the observer, diffraction rings are discernible if the diameter of the particles is large compared with the wave-length of the light. By measuring the radius of the diffraction ring, the diameter of the particles can be determined from the following equation (reference can be made to any optics text, e.g. Woods [36], or to Kuehn [37] for an explanation of the diffraction phenomena and a derivation of this equation):

$$d = \frac{\lambda \ell}{R}$$

where

d = diameter of particles

λ = wave-length of light

ℓ = distance of point source of light from particles

R = radius of diffraction ring.

If the diameter of the particles is not uniform, the diffraction ring will not be sharp and its radius will represent, in this case, the average diameter of the particles.

This technique was used in tests, discussed in Part IV, in the small Laval nozzle, the Transonic Wind Tunnel, the 2.5" Supersonic Wind Tunnel and the 12" Supersonic Wind Tunnel. In all cases no diffraction rings were observed, indicating that the droplets formed in the spontaneous condensation process are smaller than or, at the most, of the same order as the wave-length of the light.

When the valve at the inlet to the stagnation chamber of the Laval nozzle (see Fig. 5a) was closed almost instantaneously, the stagnation temperature dropped momentarily about 10° F. and droplets were observed flowing through the subsonic, as well as the supersonic, sections of the nozzle. These droplets, when observed in the supersonic section, did produce diffraction rings. The radius of the diffraction ring was 1 cm., with the point source of about 5,000 Å wave-length located at a distance of 167.5 cm. from the center of the nozzle. The droplet diameter was thus calculated to be 83.3×10^{-4} cm. A number of droplets were caught under the

same conditions by the "sample-catch" technique, to be described subsequently, and their diameters were found, by microscopic measurements, to vary between 80 and 85 x 10^{-4} cm. A fairly accurate check was thus afforded of the diffraction ring technique.

It is evident from these results that the diffraction ring technique is of quantitative value only in cases of extreme droplet size.

C. The "Sample-Catch" Technique

In this technique, the droplets are allowed to impinge on a plate coated with Magnesium-Oxide, Carbon Black, or some other suitable material. If the MgO coating is thicker than the largest drops to be caught, the impinging droplet leaves a crater on the surface of the coating that is the same diameter as that of the droplet. Hence, measurements are easily made of droplet diameters and concentration of droplets.

Unfortunately, these coatings are blown away in air of even moderate subsonic velocity and hence some method of circumventing this must be devised. One such method is to house the coated plate in a stagnation probe having a shutter at the entrance that can be opened momentarily. This technique has not been tried as yet at supersonic speeds and hence its feasibility is still open to question.

In the tests described in the section on the diffraction ring technique, the Laval nozzle exhausts into the atmosphere, making it possible to pass the coated plate rapidly across the jet.

The velocity in the jet in these tests, although still quite high, was low enough to allow easily measurable samples to be taken.

When carbon black is used as a coating, the impinging droplets do not leave a crater at the surface but spread out on impact, leaving a circular pattern in the coating. The equations have been derived for determining the original droplet diameter from the impact pattern, but such a procedure seems unduly complicated. Hence the MgO coating technique is to be preferred.

It is planned to exploit this "sample-catch" technique further since it is the only method known at the present time for determining the size and concentration of droplets uniquely. Thus, a direct check could be made of the radius and number of droplets as determined by the combination of the pressure distribution and light scattering measurements.

D. Infra-Red Absorption Technique

At the inception of this research program, a new technique was partially developed for studying the high speed flow of humid air. This technique consists in the measurement of the percentage absorption of infra-red radiation by the water vapor present in the flowing air. From such a measurement the density of the water vapor, and therefrom the air density, can be determined provided no products of condensation are present. If condensation has occurred, the Raman effect can presumably be used to determine the amount of condensation in the light path and to distinguish

liquid droplets from ice particles. Although this method is still in the developmental stages, it is believed to be of sufficient interest and to possess such potentialities as to warrant its inclusion in this report.

Certain bands in the infra-red region of the electromagnetic spectrum exhibit extremely strong absorption by the H_2O molecule. Those bands that lie in the near and photographic infra-red (0.9 to 6.5 μ) are utilized herein because they are amenable to measurement without elaborate experimental equipment, as well as the fact that their absorption by the water vapor molecule is still very intense.

The disposition of charge among the atoms in the water vapor molecule is such that the hydrogen atoms have an excess of positive charge while the oxygen atom has an excess of negative charge. Thus, a vibration of the atoms is accompanied by a change in the dipole moment, which results in the vibration spectrum of the molecule. The intense infra-red absorption region of interest is due to the fundamental vibration frequencies and their harmonics and overtones. (For a detailed treatment of infra-red and Raman spectra, reference should be made to Herzberg[38], Ruark and Urey[39], etc..)

The water vapor molecule, being tri-atomic, has 3 vibrational degrees of freedom. The corresponding normal modes of vibration have been determined by several different techniques and may be

illustrated graphically as follows:

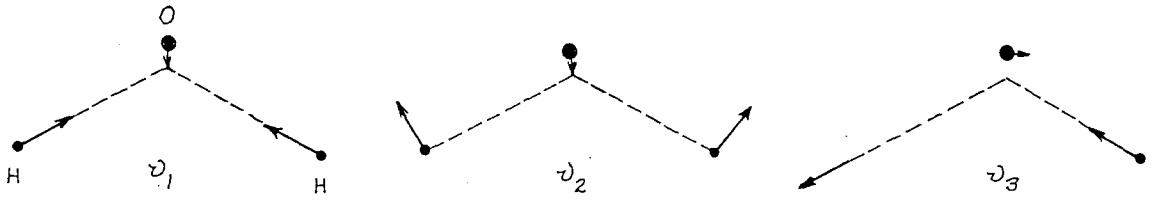

Only two of the normal modes are directly observed in the infra-red: ν_2, occurring at 6.26 μ and corresponding to the angular deformation frequency of the H-O-H molecule and ν_3, at 2.66 μ, corresponding to an anti-symmetric O-H valency vibration. The symmetric valence vibration, ν_1, occurring at 2.8 μ, exhibits intense Raman scattering only.

It was desired, in the present investigation, to pass the infra-red radiation through the Schlieren windows of the wind tunnel and measure the resulting absorption by the water vapor in the air. This necessitated the use of infra-red wave-lengths shorter than 2.5 μ, since glass does not transmit wave-lengths longer than this value. Accordingly, those harmonics and overtones of the fundamental vibration frequencies that occur at 1.87, 1.4 and 1.13 μ were investigated in an effort to determine the feasibility of employing these bands in the determination of the water vapor density.

Unfortunately, a satisfactory method for obtaining a monochromatic light source of the proper wave-length and with sufficient intensity could not be found. As a result, it was necessary to use a 500 watt signaling lamp with an infra-red filter that cut off those wave-lengths shorter than 0.9 μ and longer than

2.5 μ . This arrangement furnished an intense infra-red beam, but one that was far from monochromatic. The radiation was passed through the wind tunnel, normal to the air flow, and the intensity then measured by means of a Moll-type microthermopile, which was connected to a D'Arsonval galvonometer.

A galvanometer deflection of 30 cm. was obtained when the free-stream Mach number of the flow, through which the radiation was passed, was increased from 0 to 0.7. The heating up of the wind tunnel walls, however, resulted in a marked zero shift, which, coupled with additional extraneous radiation, made the readings unreliable. Nevertheless, in spite of the fact that a monochromatic source was not used, the feasibility of the technique seems established.

An attempt to utilize an infra-red telescope, in place of the microthermopile, to obtain a qualitative picture of the density field over an airfoil in the wind tunnel met with no success. This is believed to be due to the fact that the intense absorption bands beyond 1.3 μ were beyond the cut-off wave-length of the infra-red telescope used. Furthermore, the light path through the water vapor was very short (5 cm.) and the sensitivity of the telescope to the small changes in light intensity is not known. It is quite possible, however, that some of the new infra-red radiation receiving cells that have a cut-off limit of 2 to 3 μ may prove of value for such a qualitative observation of the density field.

REFERENCES

1. von Helmholtz, R.: Annal. d. Phys. (1887), Vol. 32, p. 1

2. Wilson, C.T.R.: Phil. Mag. (1897), Vol. A 189, p. 281; Proc. Roy. Soc. London (1897), Vol. 61, p. 240.

3. Powell, C. F.: Condensation Phenomena at Different Temperatures. Proc. Roy. Soc. of London (A), (1928), Vol. 119, p. 553.

4. Sander and Damköhler: Übersättigung bei der spontanen keimbildung in Wasserdampf. Naturw., (1943), Vol. 31, p. 460.

5. Cwilong, B.M.: Sublimation in a Wilson Chamber. Proc. Roy. Soc. of London (A), (1947), Vol. 190, p. 137.

6. d'Albe, Fournier: Condensation of Water Vapor Below 0°C. Nature, (1948), Vol. 162, p. 921.

7. Stodola, A.: Steam and Gas Turbines. McGraw-Hill Book Company, Inc. (1927), Vol. II, p. 117; Vol. D, p. 1060.

8. Yellott, J. I.: Supersaturated Steam. - Engineering, (1934), Vol. 137, pp. 137 and 303.

9. Yellott, J. I. and Holland, C. K.: The Condensation of Flowing Steam - Condensation in Diverging Nozzles. Engineering, 1937, Vol. 143, pp. 647 and 703.

10. Rettaliata, J.T.: Undercooling in steam nozzles. Trans. A.S.M.E., (1936), Vol. 58, p. 599.

11. Binnie, A.M. and Woods, M.W.: The pressure Distribution in a Convergent-Divergent Steam Nozzle. Proc. Inst. Mech. Eng., (1938), Vol. 138, p. 229.

12. Hermann, R.: Der Kondensationsstoß in Überschall-Windkanaldüsen. Z.A.M.M. (1942), Vol. 19, p. 201; also R.T.P.Translation No. 1581.

13. Oswatitsch, Kl.: Kondensationerscheinungen in Überschallendüsen, Z.A.M.M. (1942), Vol.22, p.1; also R.T.P.Translation No.1905.

14. Oswatitsch, Kl.: Die Nebelbildung in Windkanälen and ihr Einfluß auf Modellversuche. Jahrbuch der L.F.F. (1941), p. 692; also Reports and Translations No. 459.

15. Charyk, J.V.: Condensation Phenomena in Supersonic Flow. Ph.D.Thesis, California Institute of Technology (1946).

16. Burgess, W.C. and Seashore, F.L.: Criteria for Condensation-Free Flow in Supersonic Tunnels. NACA Report (To be published).

17. Redington: An Investigation of Condensation Phenomena in a Small Supersonic Nozzle. Cornell Aeronautical Laboratory Report No. AF-390-A-7 (1946).

18. Epstein, P.S.: Textbook of Thermodynamics. John Wiley and Sons, Inc. (1937).

19. Gibbs, J.W.: The Scientific Papers of J.Willard Gibbs. Longmans, Green and Co. (1906). Vol. 1.

20. Volmer, M.: Kinetik der Phasenbildung. Chemische Reaktion. Vol. IV. K.F.Bonhoeffer (1939).

21. Zeldovich,J.: Journal of Experimental and Theoretical Physics (USSR), (1942), Vol. 12, p. 525.

22. Becker, R. and Döring,W.: Kinetische Behandlung der Keimbildung in übersättigen Dampfen. Annalen der Physik (1936), Vol. 24, p. 719.

23. Volmer, M. and Weber, A.: Keimbildung in Übersattigen Gebilden. Zeitschr. f. phys, Chem. (1926), Vol. 119, p. 277.

24. Farkas, L.: Keimbildungs geschwindigkeit in übersättigen Dampfen. Zeitschr f. physik. Chem.(1927), Vol.125,p.236.

25. Stranski, I. and Kaischew, R.: Zur Kinetischen Ableitung der Keimbildungsgeschwindigkeit. Zeitschr. f. physik. Chem. (1934), Vol. 26, p. 317.

26. Frenkel, J.: Kinetic Theory of Liquids. Oxford Press (1946).

27. Tolman, R.C.: Effect of Droplet Radius on Surface Tension. J.Chem. Phys., March 1949.

28. Washburn, E.W.: International Critical Tables. McGraw-Hill Book Co., Inc. (1926).

29. Lord Rayleigh: Phil.Mag. (1871), Vol. 41, pp. 107 and 274.

30. Einstein, A.: Investigations on the Theory of the Brownian Movement. E.P.Dutton and Company, p. 49.

31. Langmuir, I. and Blodgett, K.: A Mathematical Investigation of Water Droplet Trajectories. Army Air Forces Technical Report No. 5418 (1946).

32. Samaras, D.G.: Gas Dynamic Treatment of Exothermic and Endothermic Discontinuities. Canadian Journal of Research (1948), Vol. 26, p. 1.

33. Heybey: Analytical Treatment of Normal Condensation shock. NACA Technical Memorandum No. 1174 (1947).

34. Hicks, B.L., Montgomery, D.J. and Wasserman, R.H.: The One-Dimensional Theory of Steady Compressible Fluid Flow in Ducts with Friction and Heat Addition. NACA Adv. Restricted Report No. E6E22 (1946)

35. Liepmann, H.W. and Puckett, A.E.: Introduction to Aerodynamics of a Compressible Fluid. John Wiley and Sons, Inc. (1947).

36. Wood, R.W.: Physical Optics. The Macmillan Co. (1934)

37. Kuehn: Atomization of Liquid Fuels. NACA Technical Memorandum No. 329 (1925).

38. Herzberg, G.: Molecular Spectra and Molecular Structure. Prentice-Hall, Inc. (1939) and Infra-Red and Raman Spectra of Polyatomic Molecules, (1945) D.VanNostrand Co., Inc.

39. Ruark, A. and Urey, H.: Atoms, Molecules and Quanta. McGraw-Hill Book Co., Inc. (1930).

40. Dorsey, N.E.: Properties of Ordinary Water-Substance. Reinhold Publ. Corp. (1940).

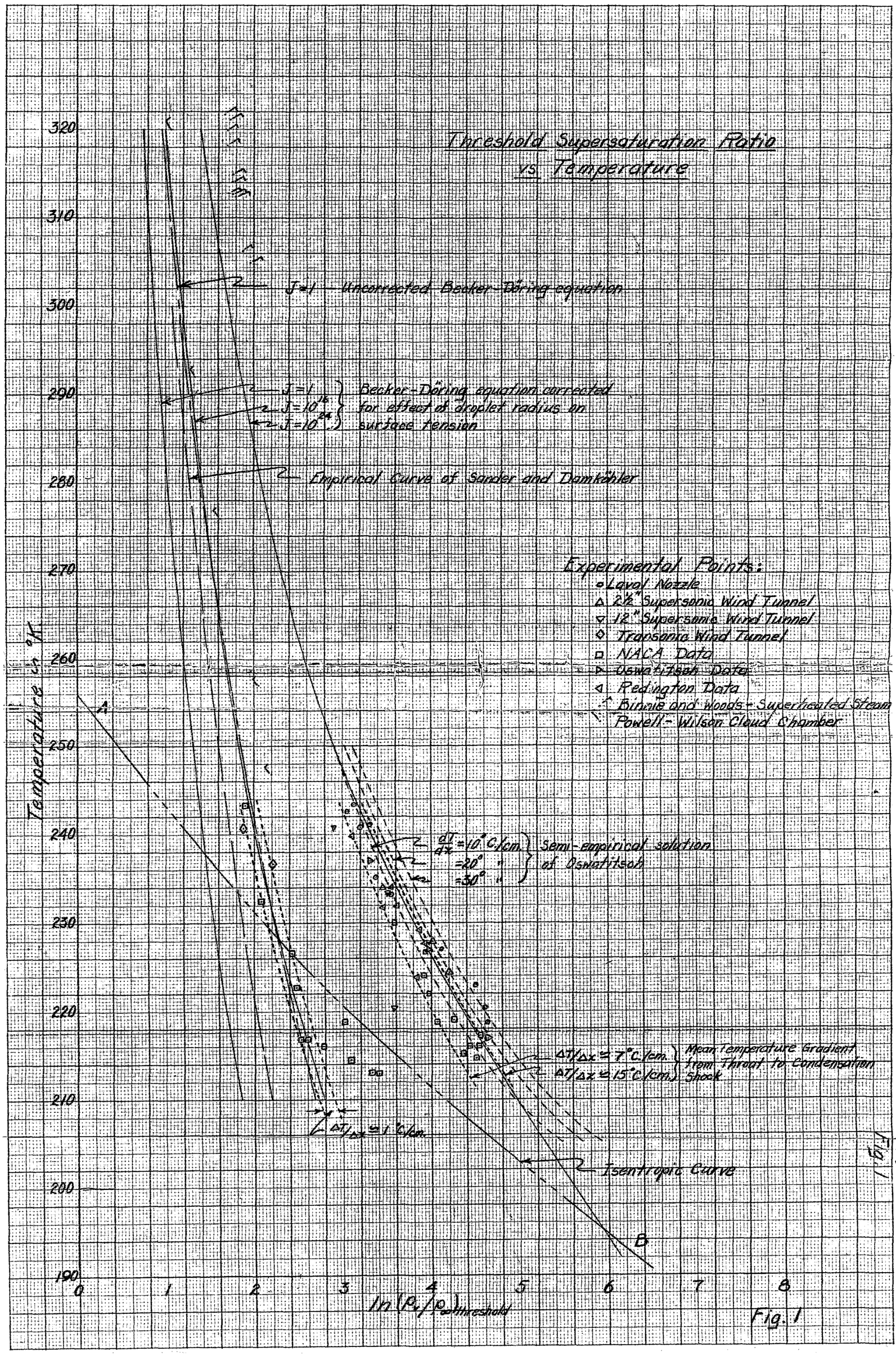
Threshold Supersaturation Ratio vs. Temperature
J=1 — Uncorrected Becker-Döring equation
Becker-Döring equation corrected for effect of droplet radius on surface tension
J=1
J=10^16
J=10^24
Empirical Curve of Sander and Damköhler
Experimental Points:
Laval Nozzle
2½" Supersonic Wind Tunnel
12" Supersonic Wind Tunnel
Transonic Wind Tunnel
NACA Data
Oswatitsch Data
Redington Data
Binnie and Woods - Superheated Steam
Powell - Wilson Cloud Chamber
dT/dx = 10° C/cm.
= 20° "
= 30° "
Semi-empirical solution of Oswatitsch
ΔT/Δx ≅ 7° C/cm.
ΔT/Δx ≅ 15° C/cm.
Mean Temperature Gradient from Throat to Condensation Shock
ΔT/Δx ≅ 1° C/cm.
Isentropic Curve
A
B
Temperature °K
320
310
300
290
280
270
260
250
240
230
220
210
200
190
0
1
2
3
4
5
6
7
8
1/2 (P_v/P_∞)_threshold

Fig. 1

Fig. 2

Variation of Rate of Increase of Supersaturation with Temperature

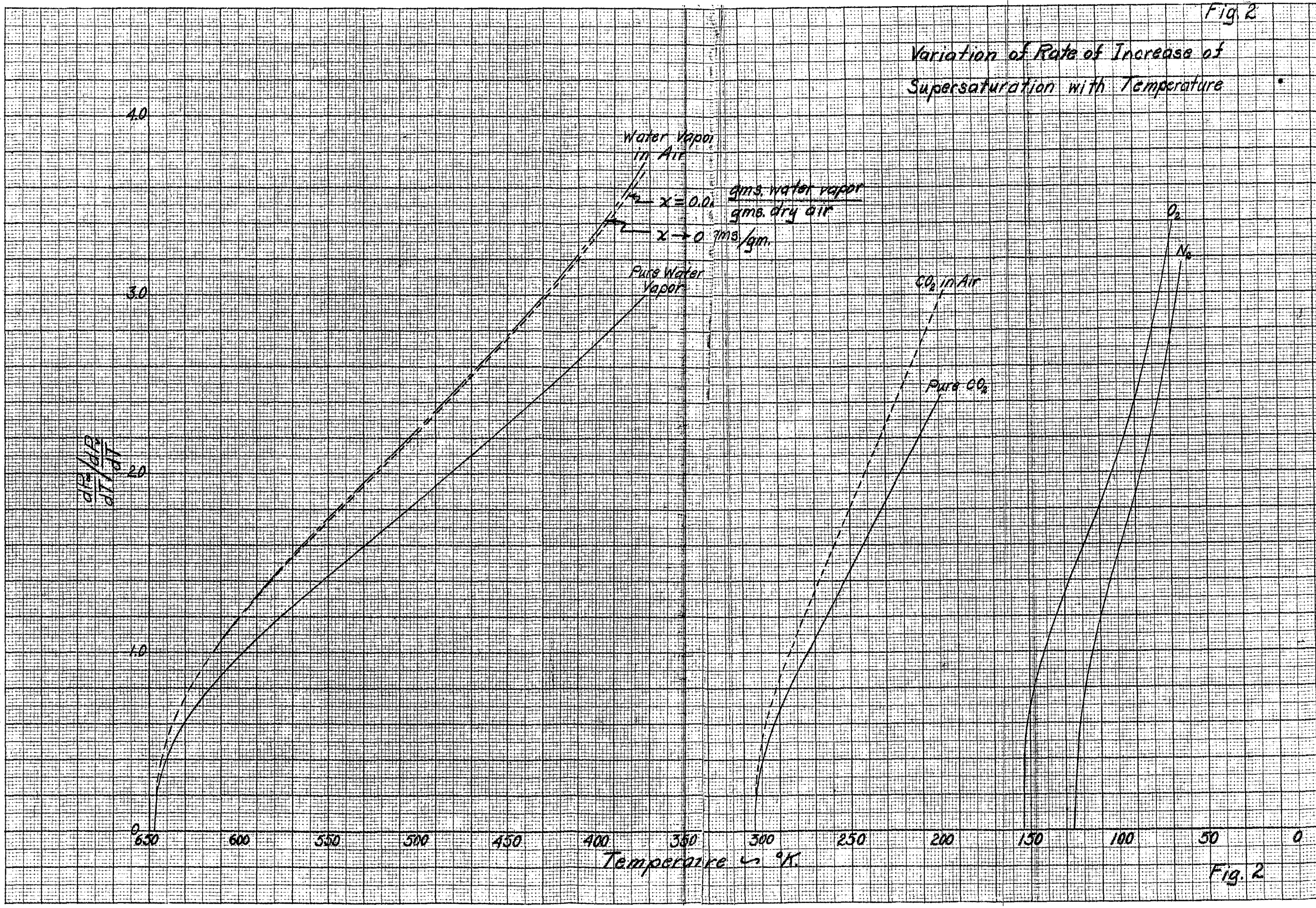

Fig. 2

Fig. 3

Variation of Radius of Characteristic Droplet with Degree of Supersaturation for Various Temperatures

P_v = Vapor Pressure
P_∞ = Saturation Vapor Pressure
——— Uncorrected for Effect of Droplet Radius on Surface Tension.
——— Corrected According to Reference (27).

$T = 213$ °K.
233
253
273
293
313

$\ln (P_v/P_\infty)$

Radius of Characteristic Droplet — cm.

Fig. 3

Fig 4

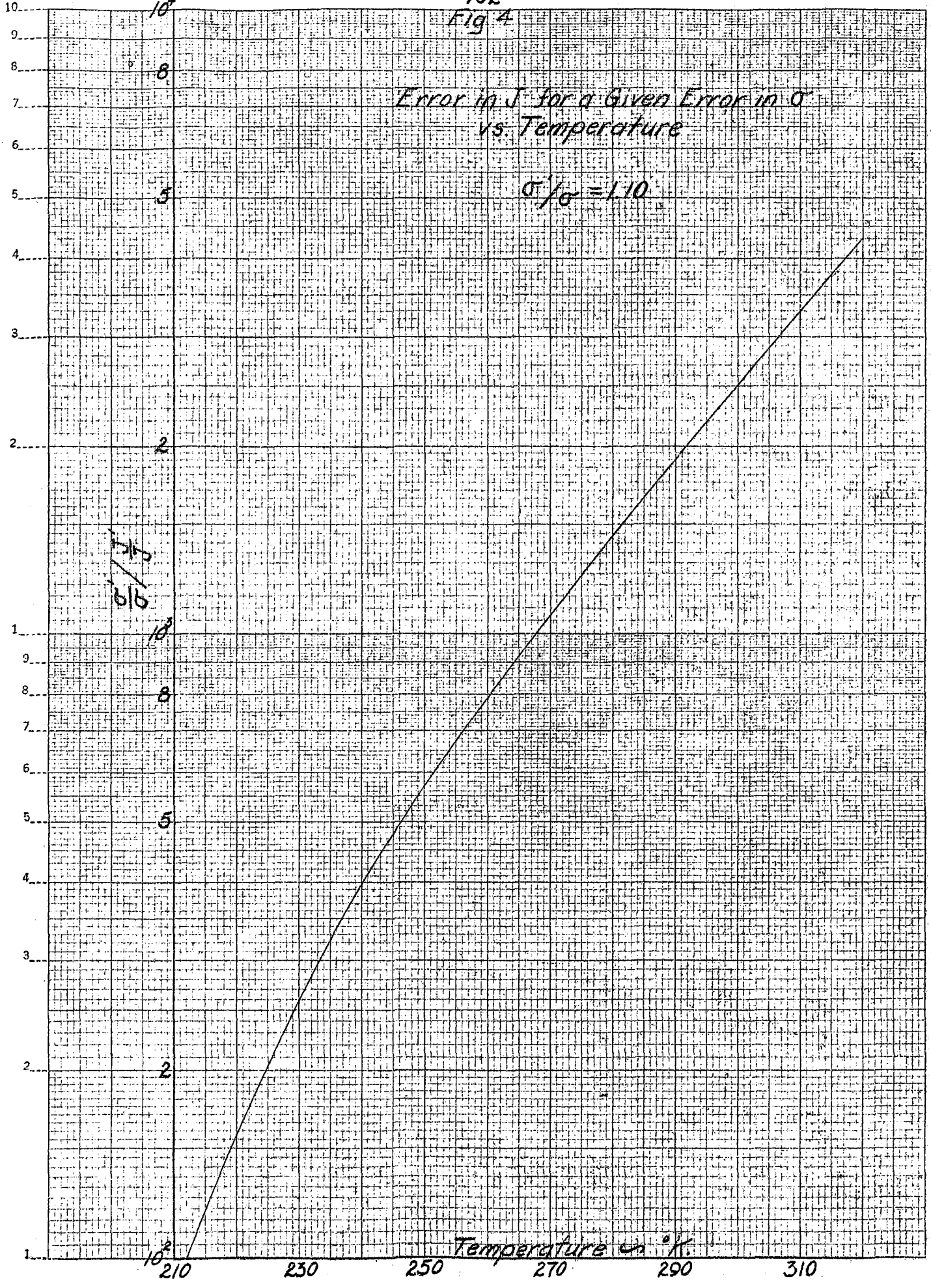
Error in J for a Given Error in σ
vs. Temperature
σ'/σ = 1.10
10⁴
8
5
2
10³
8
5
2
10²
210
230
250
270
290
310
Temperature in °K.

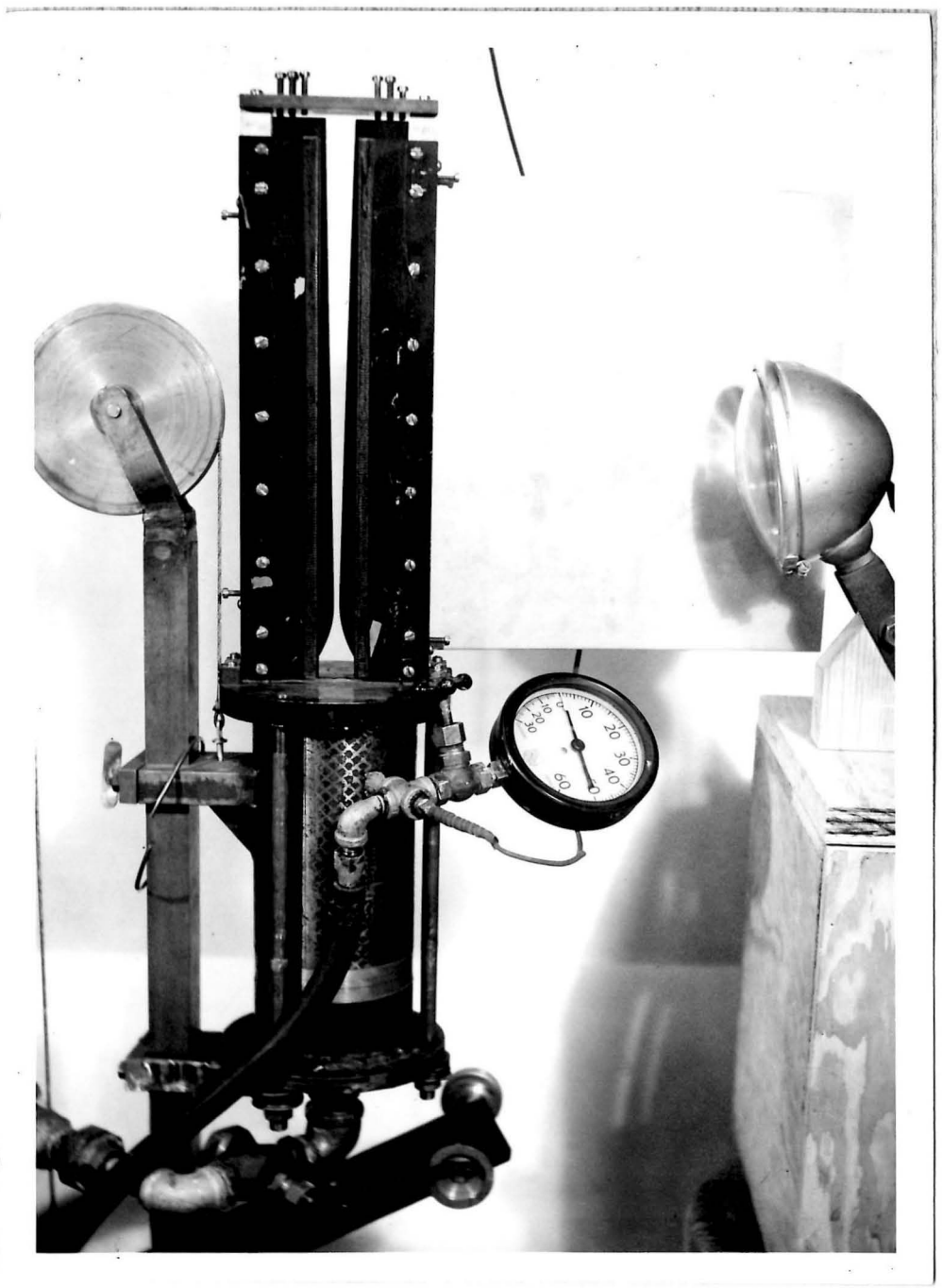

Figure 5a

Laval Nozzle Apparatus

Light Scattering Installation (Near Reflector Removed)

Figure 5b

Laval Nozzle Apparatus

Pressure Distribution Installation

Fig. 6a

Laval Nozzle
Pressure Distribution Measurements

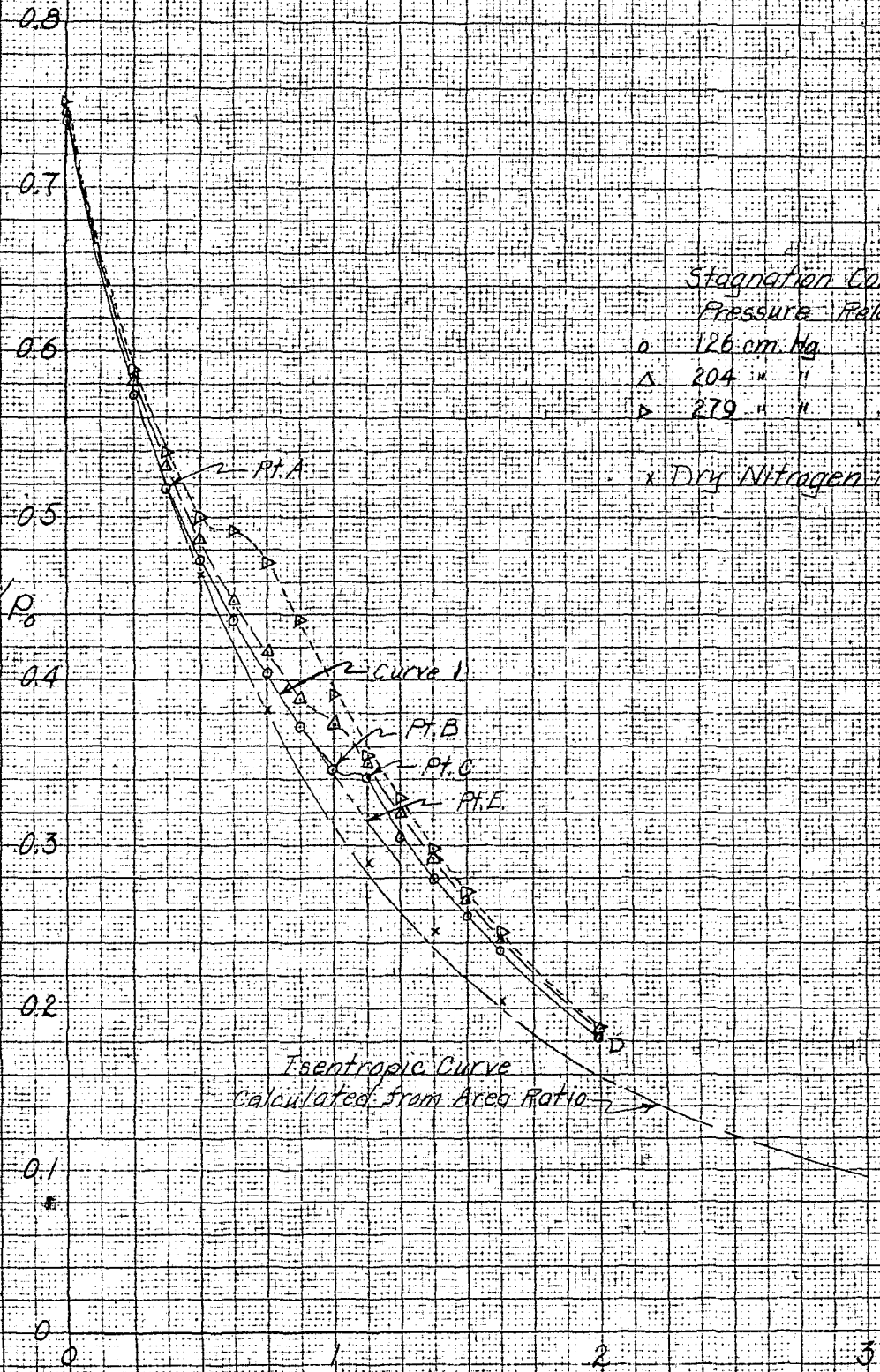

Fig. 6a

Fig. 6b

Laval Nozzle

Pressure Distribution Measurements (Cont'd.)

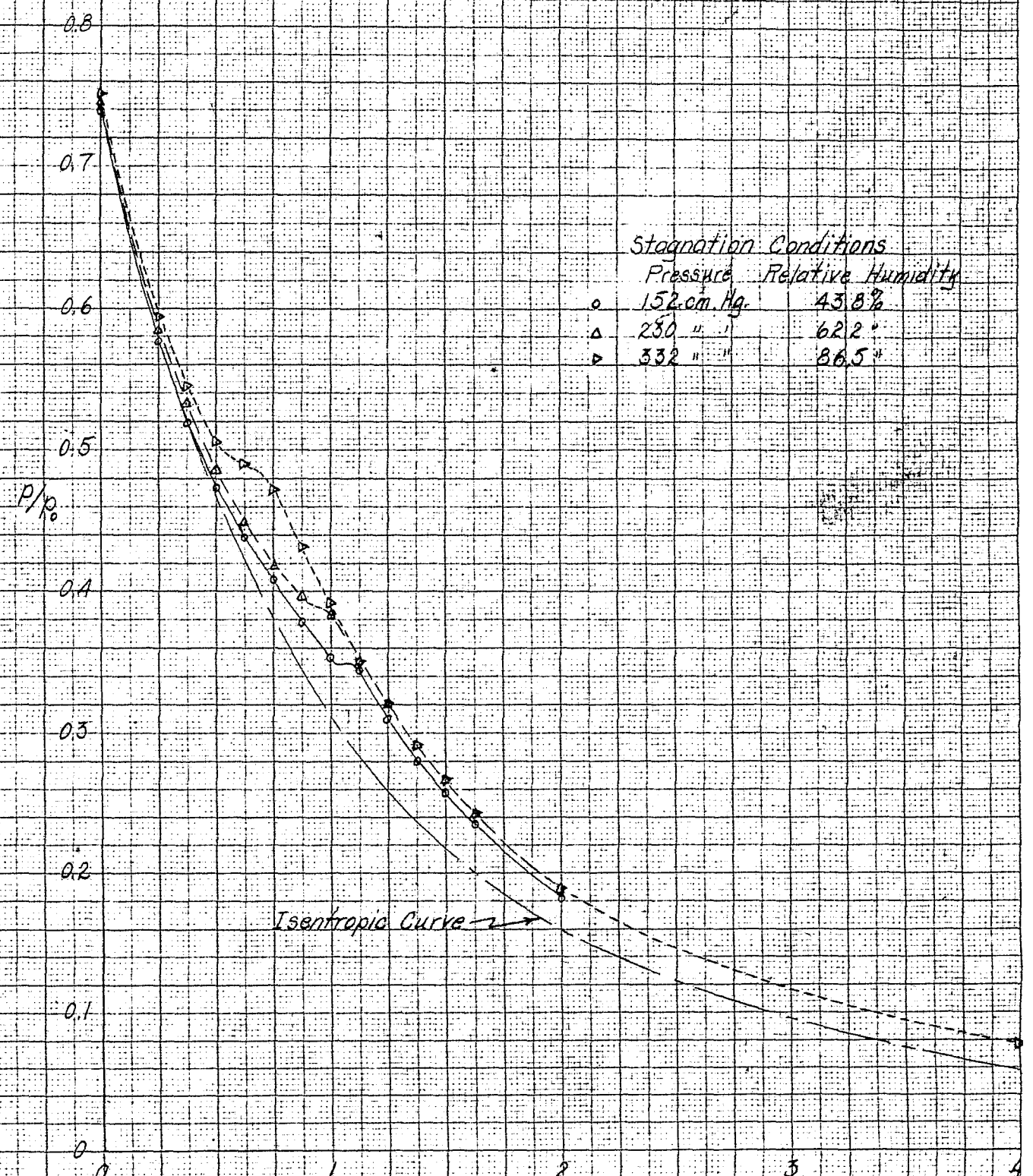

Fig. 6b

Fig. 6c

Laval Nozzle

Pressure Distribution Curves (Cont'd.)

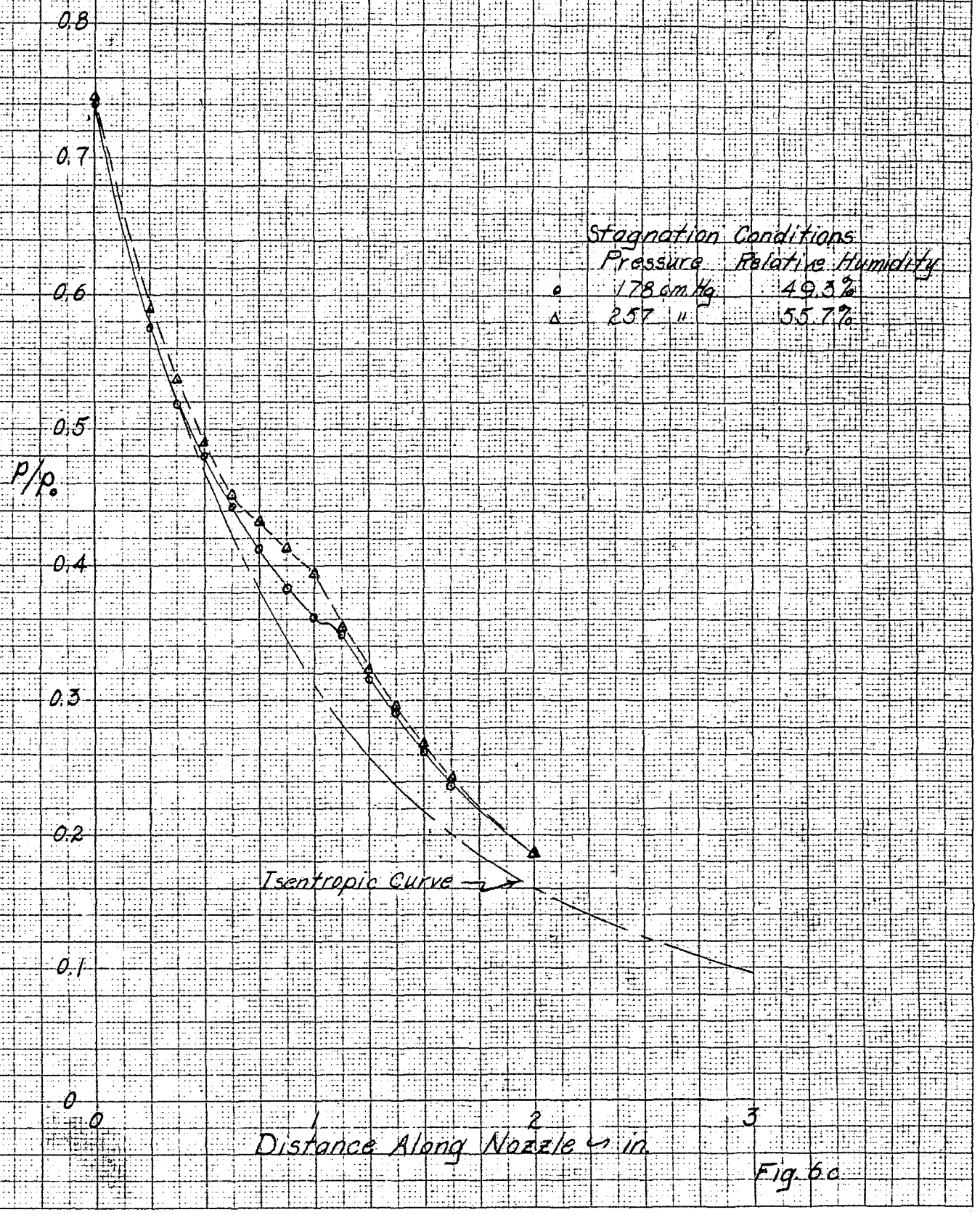

Fig. 6c

2 1/2" Supersonic Wind Tunnel Test

Representative Static Pressure Probe Measurements

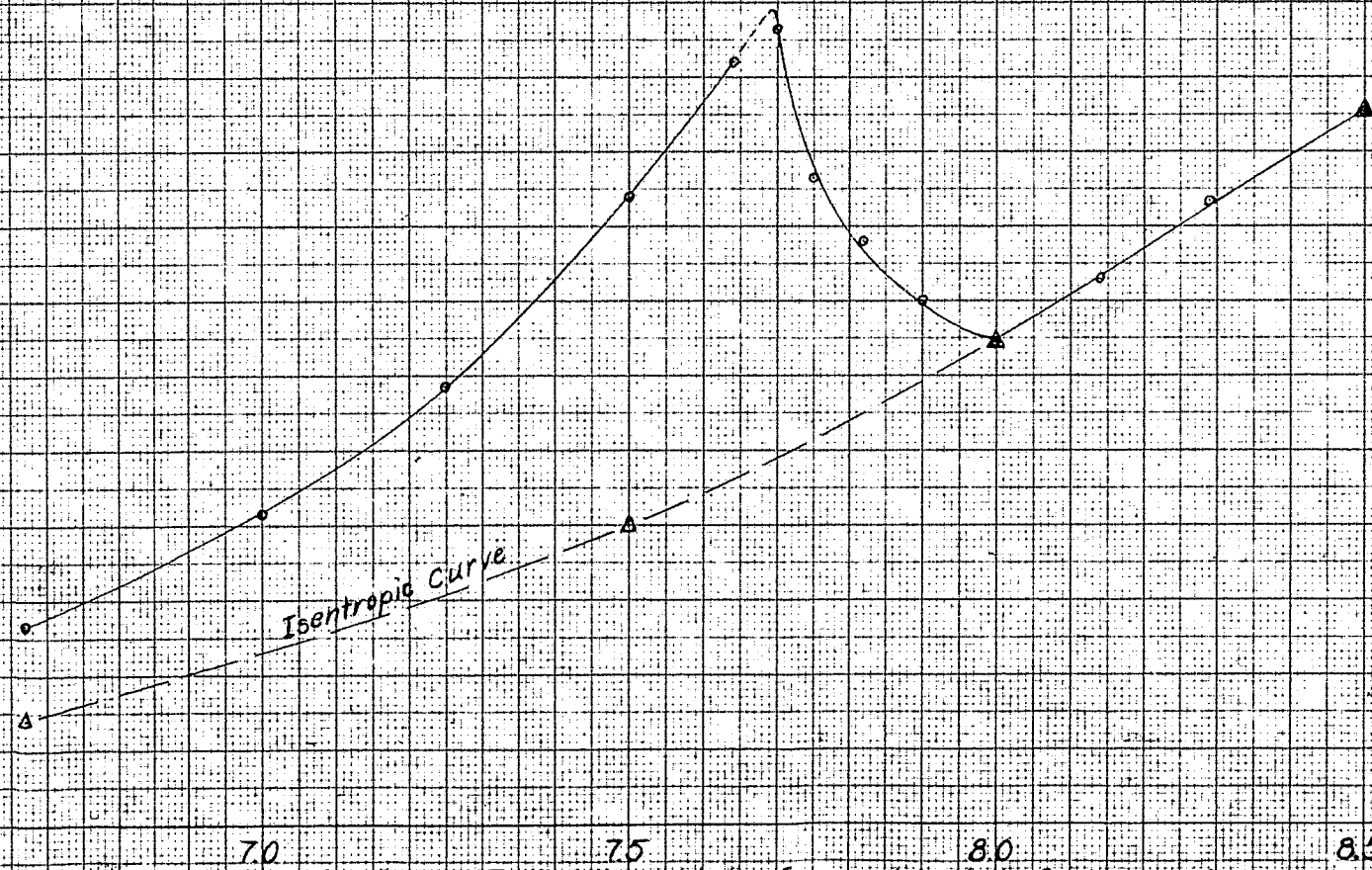

Fig. 7a

Fig. 7a


Transonic Wind Tunnel Test
Representative Static Pressure Plate Measurements
0.54
0.52
0.50
0.48
0.46
0.44
0.42
0.40
p/p₀
0
1
2
3
4
5
6
7
8
9
10
Distance Along Nozzle - in.

Fig. 7b

Fig. 7a

Mach Number 3.2 Condensation Test

Static Pressure Measured at One Station in Test Section

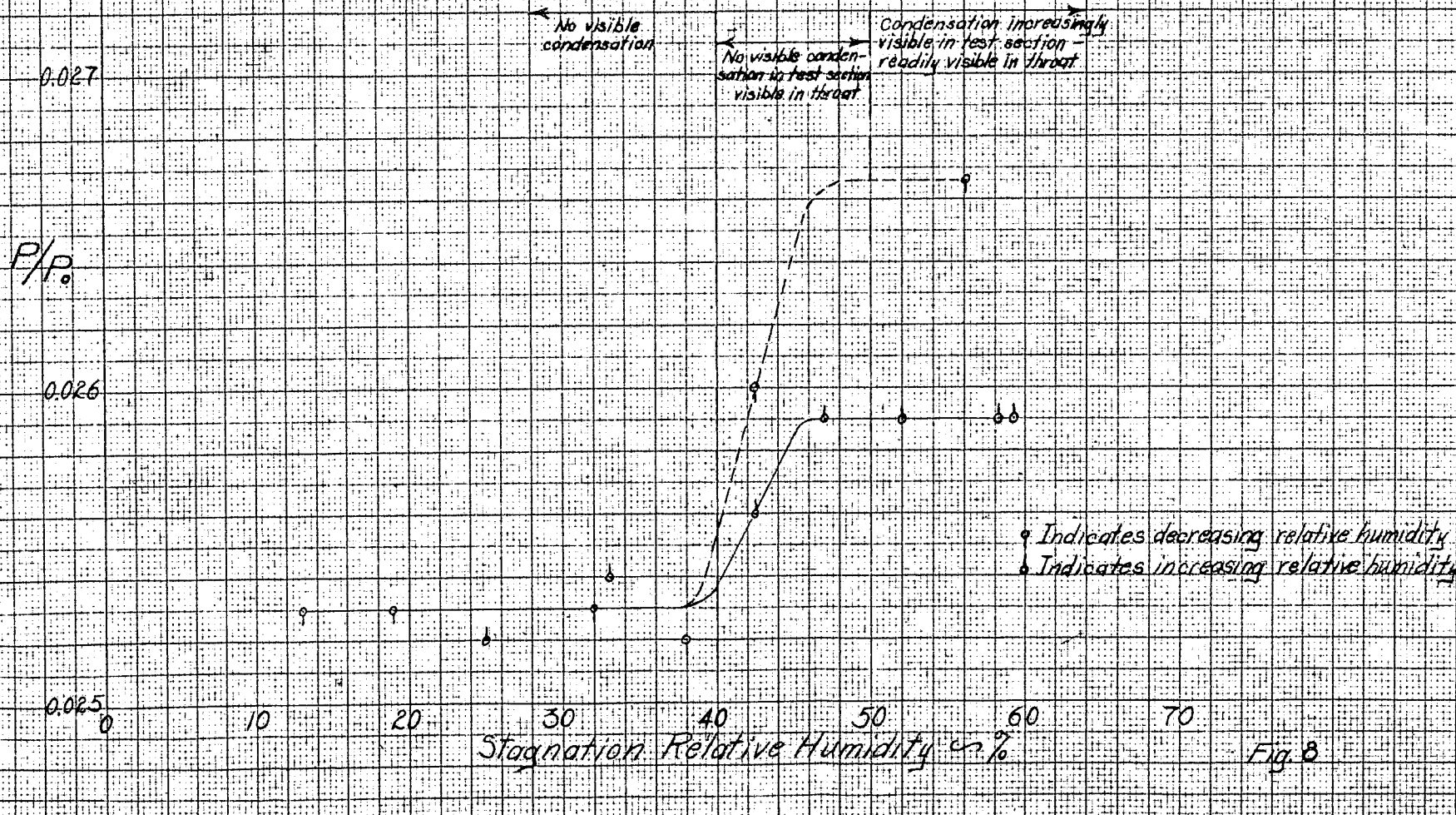

Fig. 8

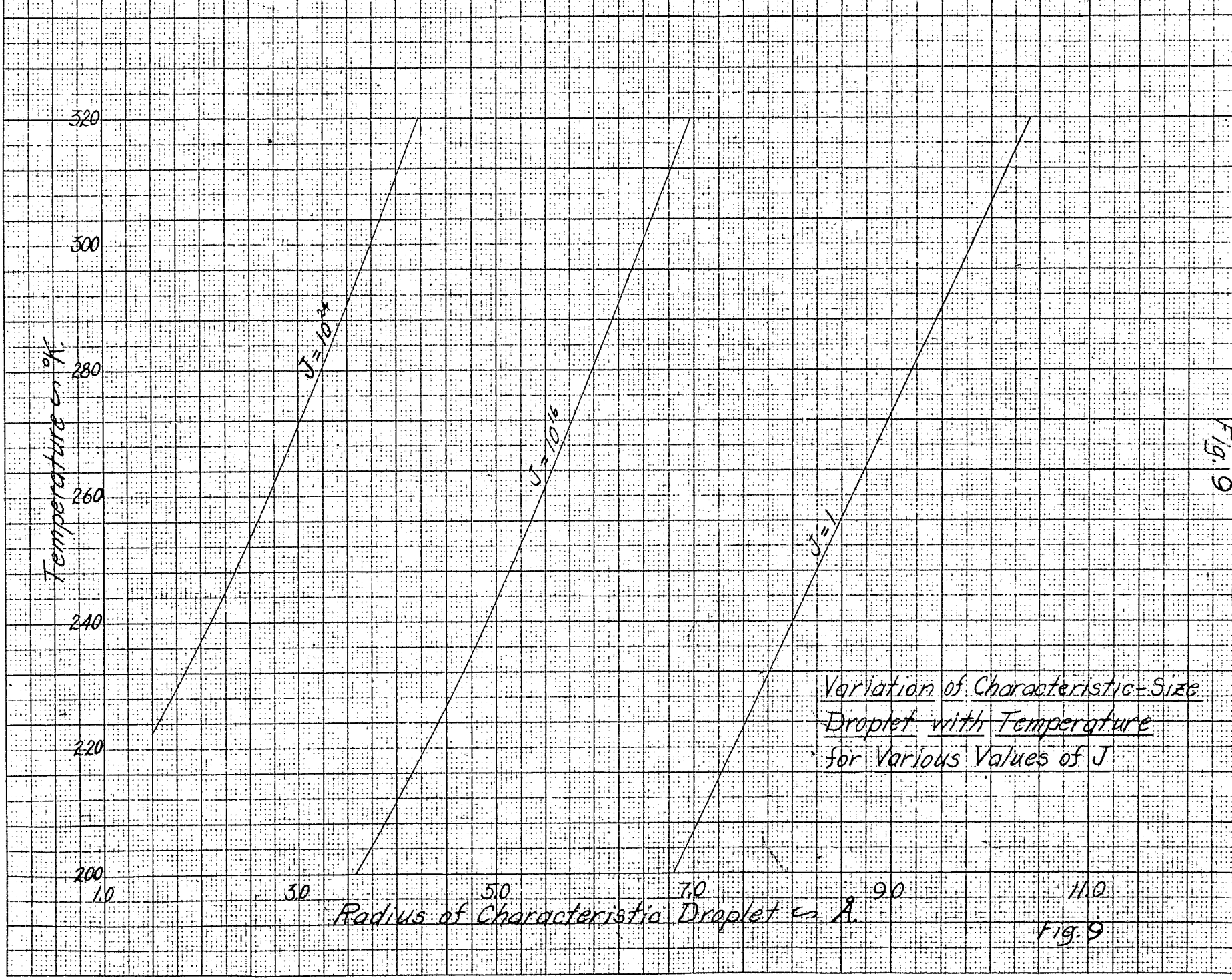

Variation of Characteristic-Size Droplet with Temperature for Various Values of J

Fig. 9

Fig. 9

Fig. 10

Error in Mach Number Determined from Oblique Shock Angle Due to Vaporization of Droplets in the Flow — For Various Wedge Half-Angles

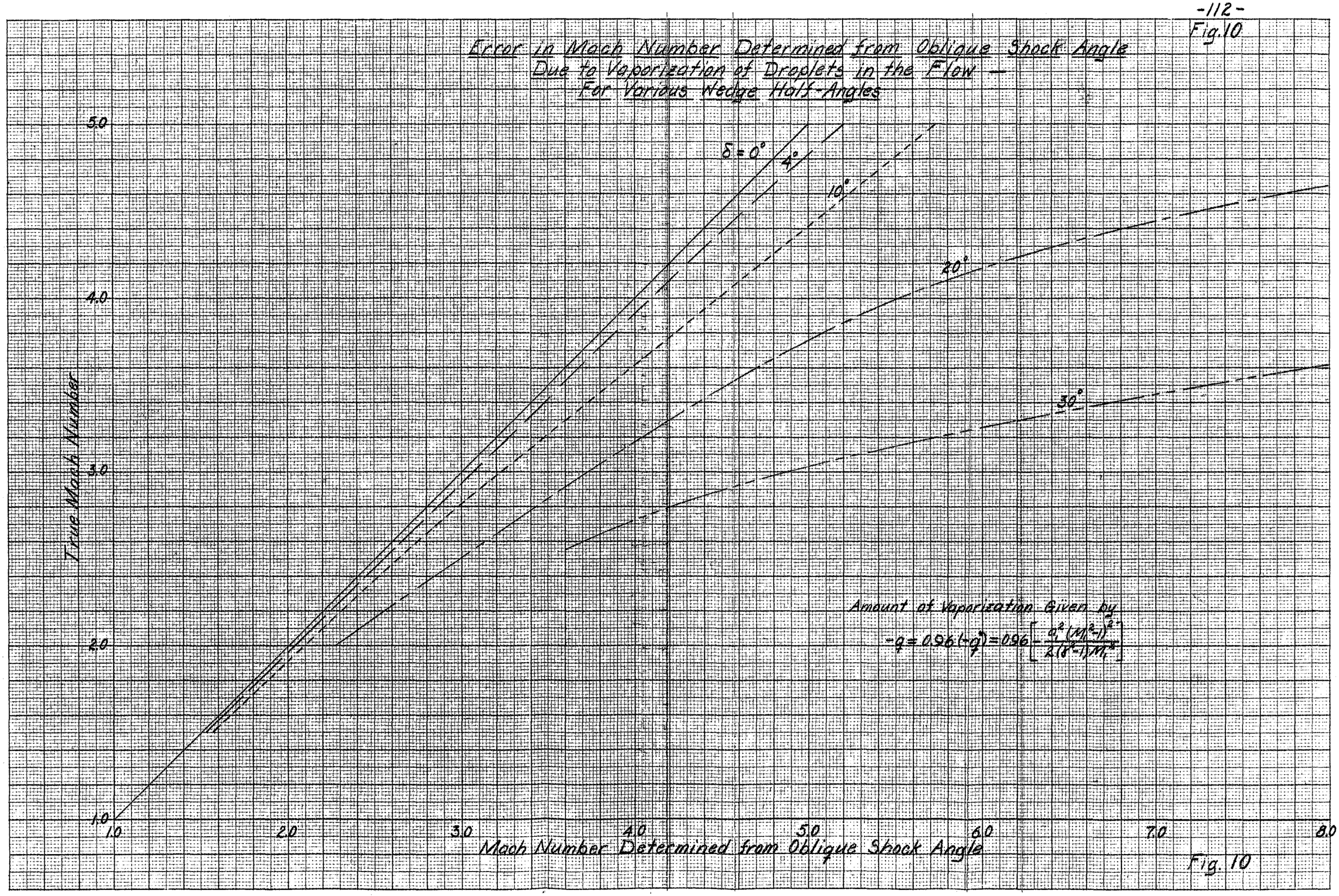

Amount of Vaporization Given by

$$-q = 0.96(-q') = 0.96\left[-\frac{a_1^2(M_1^2-1)^2}{2(\delta^2-1)M_1^2}\right]$$

Fig. 10

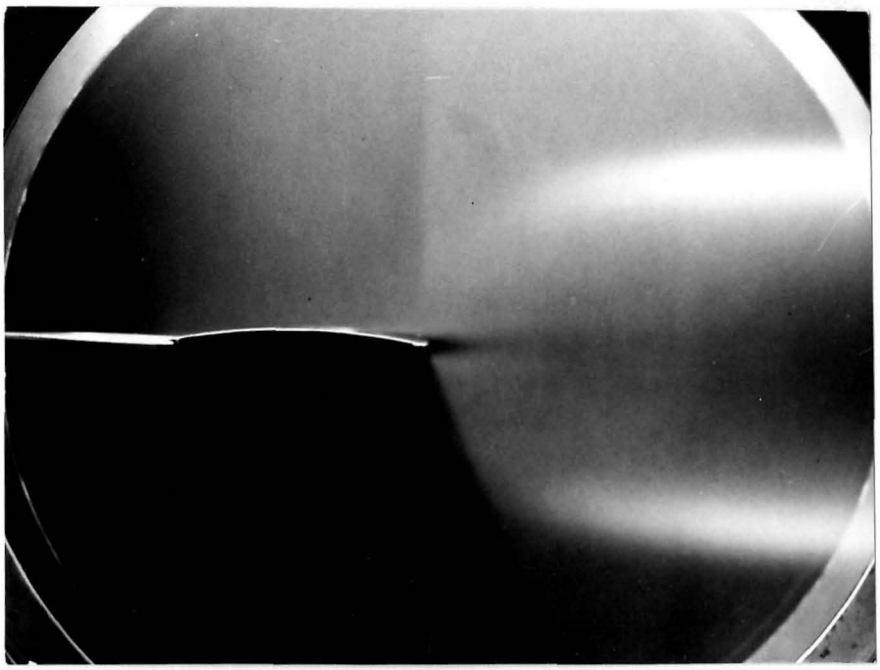

(a) Light Scattering Photograph

(b) Schlieren Photograph

Figure 11 -- Condensation Sheets Behind 12% Thick Bi-Convex Airfoil at M = 0.90 - Laminar-Boundary-Layer-Type Shock Wave

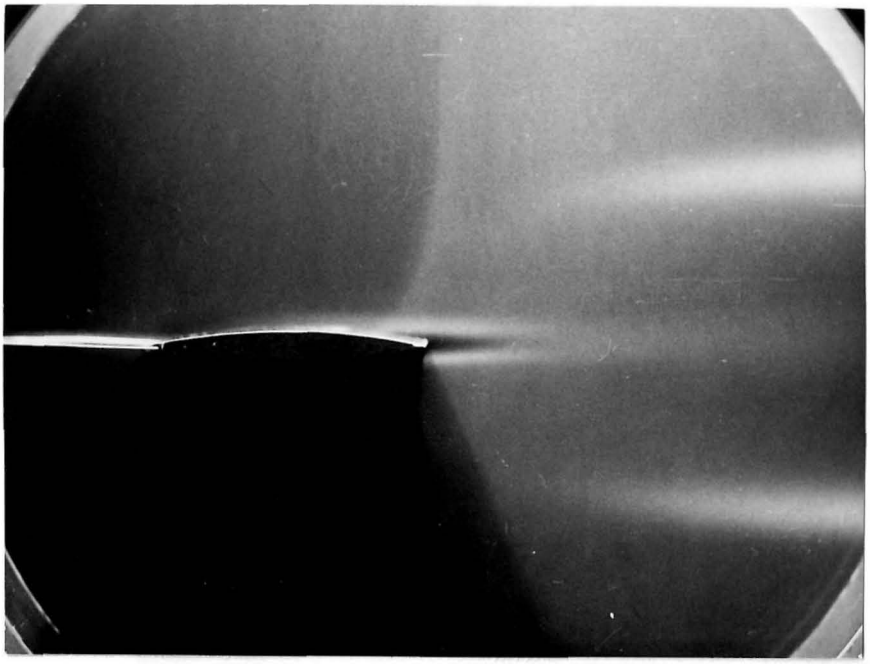

(c) Light Scattering Photograph

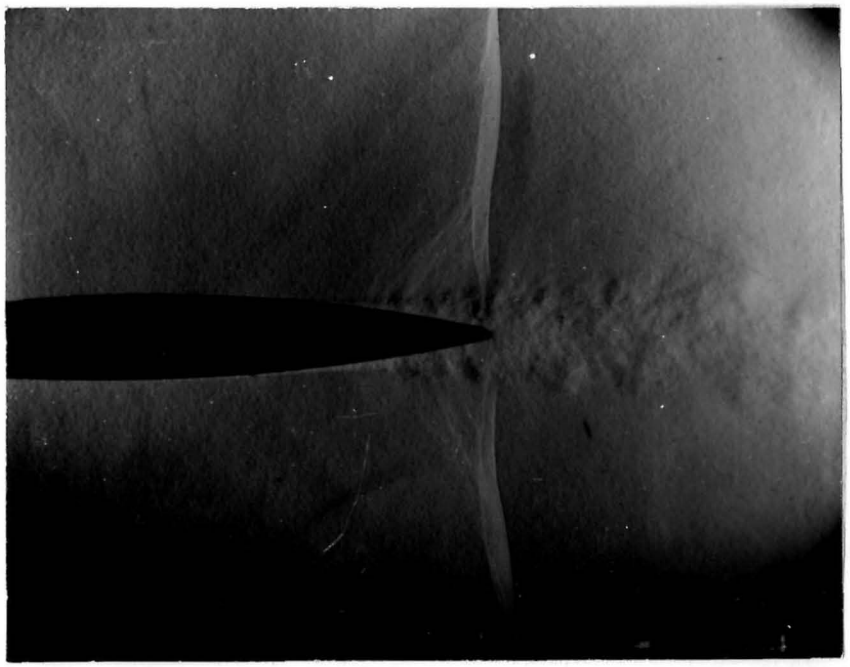

(d) Schlieren Photograph

Figure 11 (Continued) -- Turbulent-Boundary-Layer-Type Shock Wave

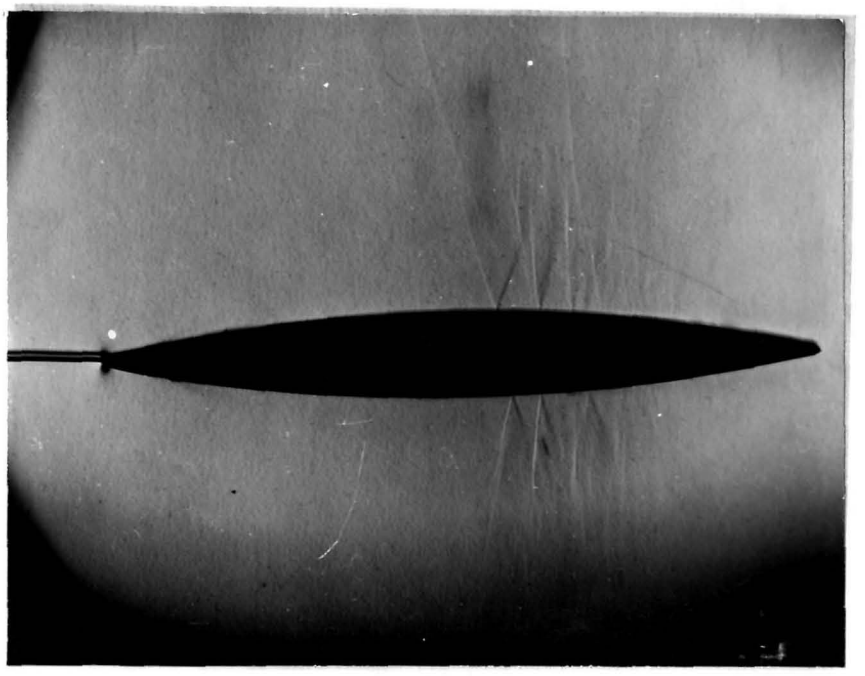

(e) No Droplets Present in Flow

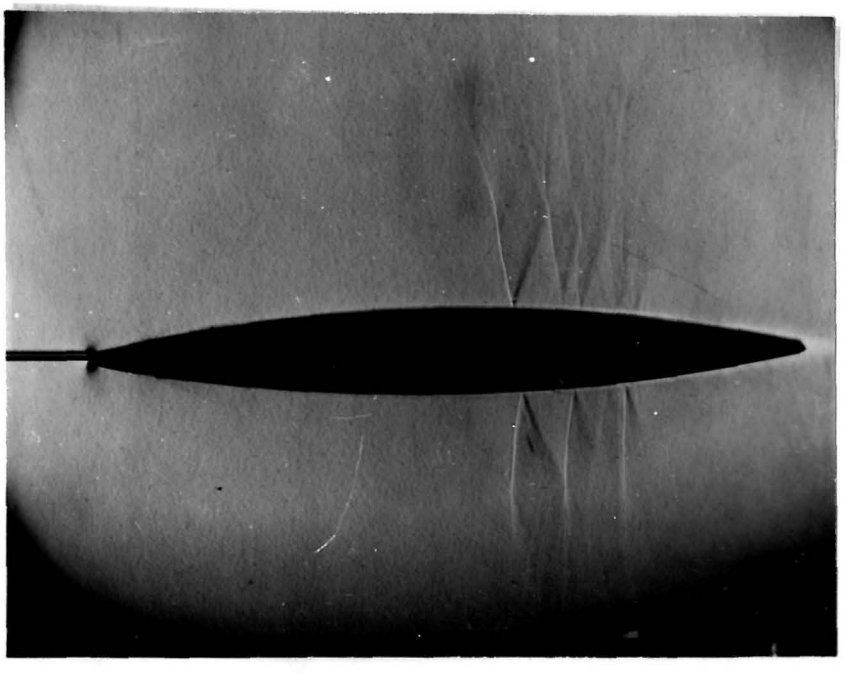

(f) Droplets Present in Flow

Figure 11 (Continued) -- Schlieren Photograph at M = 0.838

Correction Factors for Use in Appendix III.

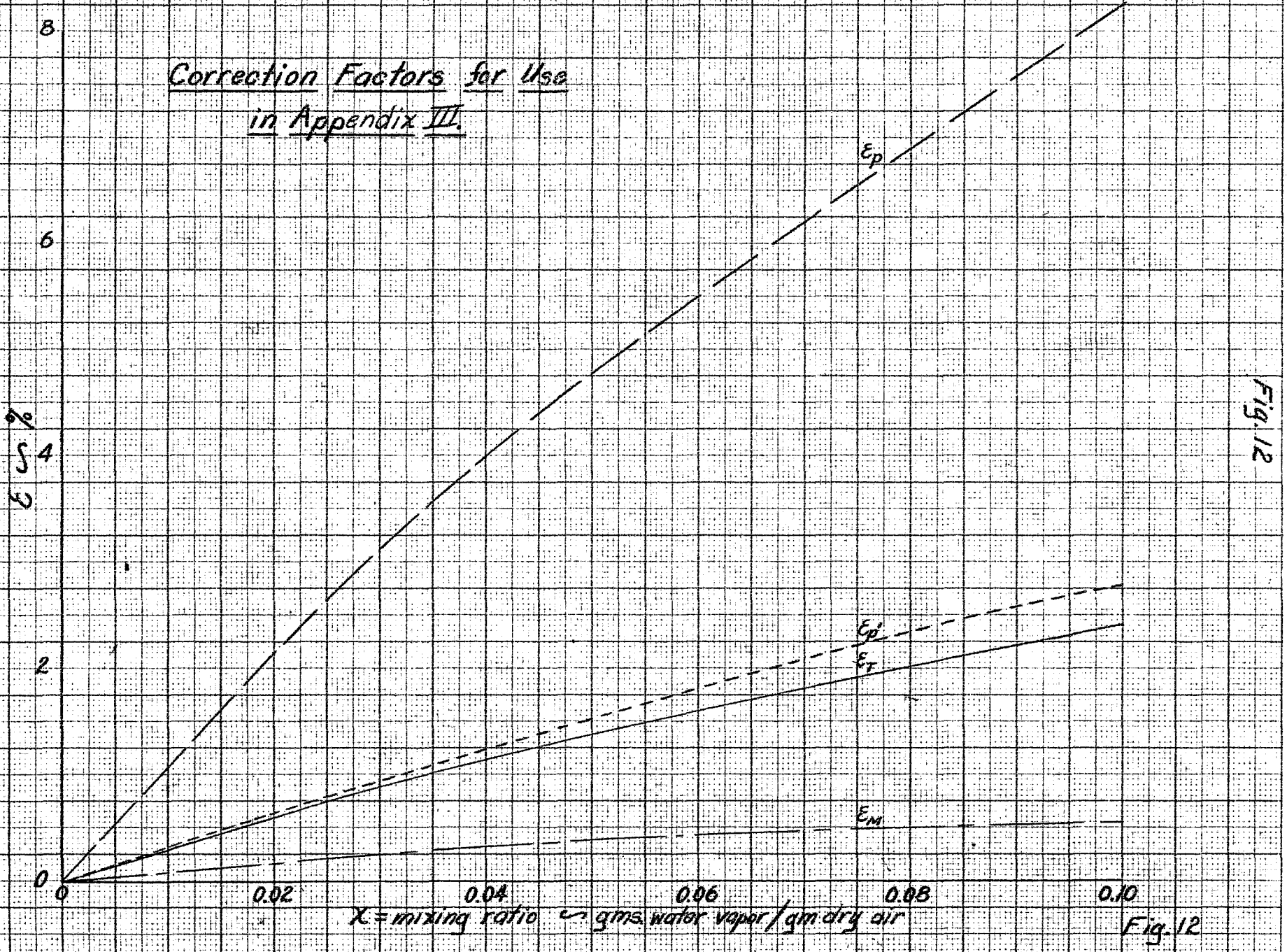

Fig. 12

Fig. 12

Fig. 13

Variation of Saturation Vapor Pressure with Temperature

——— Over Water

— — — Over Ice

Saturation Vapor Pressure — mm Hg

Temperature — °K

Fig. 13

Fig. 14

Variation of Mixing Ratio with Stagnation Pressure for Various Values of Stagnation Dew Point

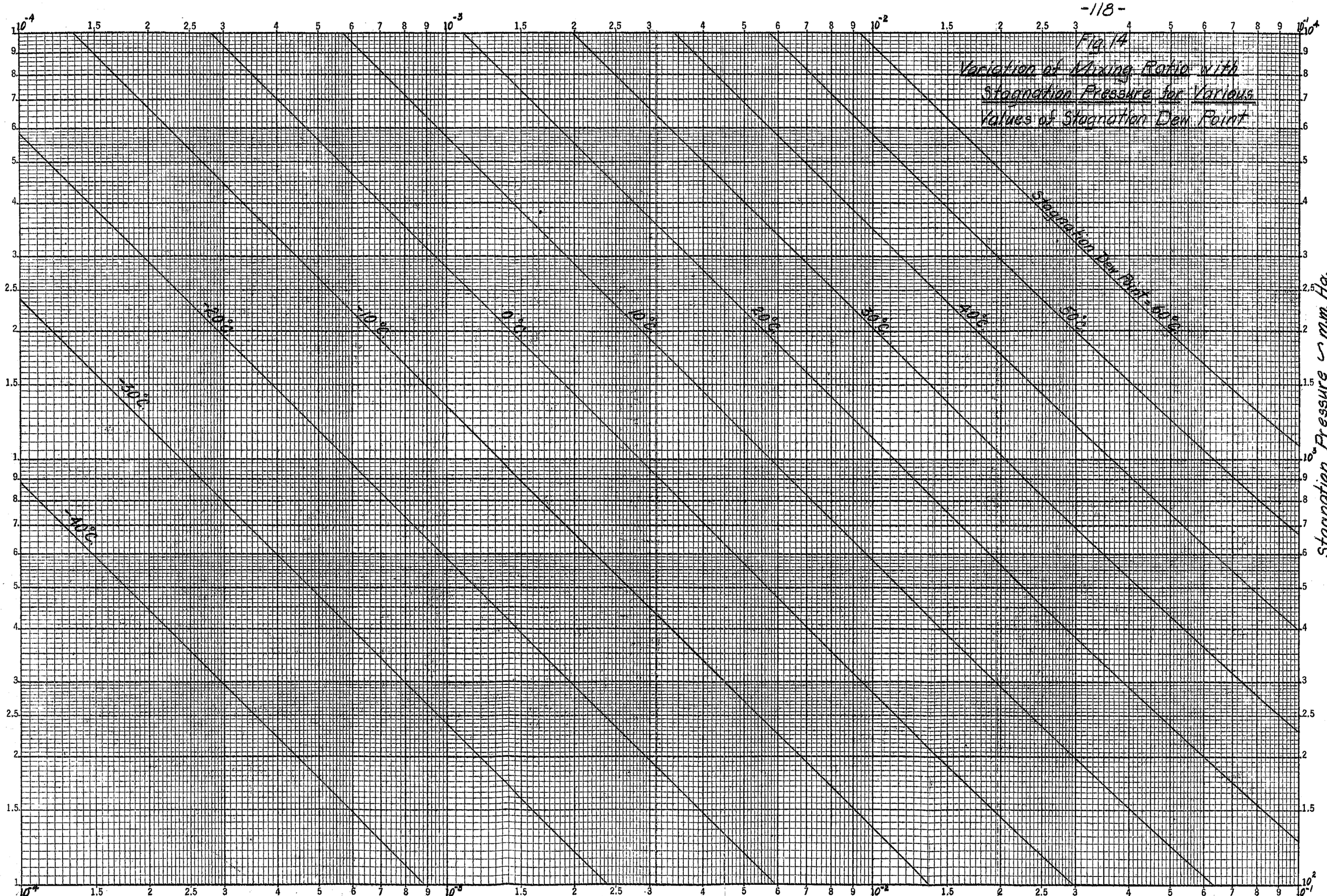

Fig. 15

Variation of Surface Tension with Absolute Temperature

— — Extrapolated

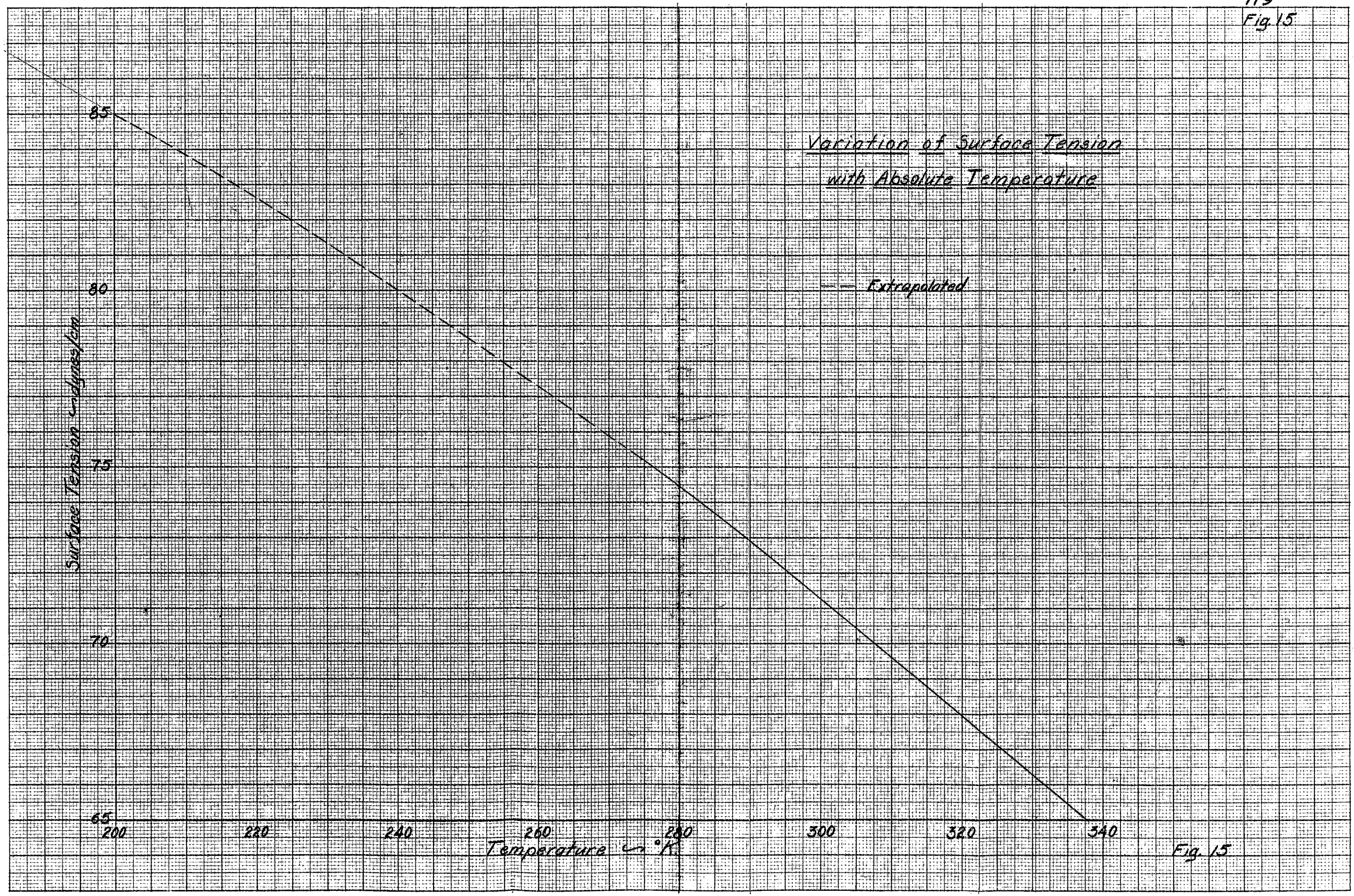

Fig. 15

Fig. 16

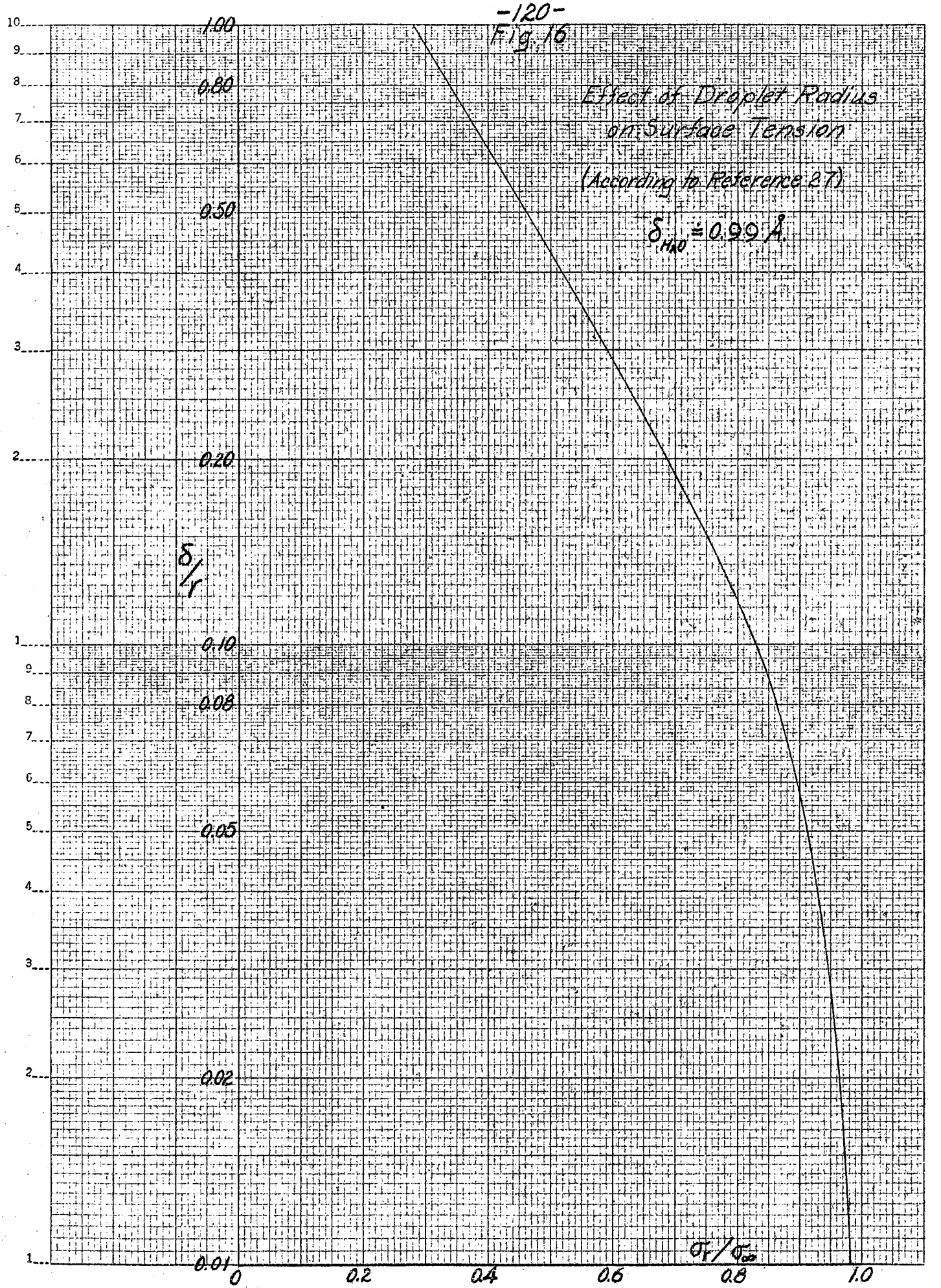
Effect of Droplet Radius on Surface Tension
(According to Reference 27)
$\delta_{H_2O} = 0.99$ Å
δ/r
σ_r/σ_∞
1.00
0.80
0.50
0.20
0.10
0.08
0.05
0.02
0.01
0
0.2
0.4
0.6
0.8
1.0

VARIATION OF RADIUS OF CHARACTERISTIC DROPLET WITH DEGREE OF SUPERSATURATION FOR VARIOUS TEMPERATURES

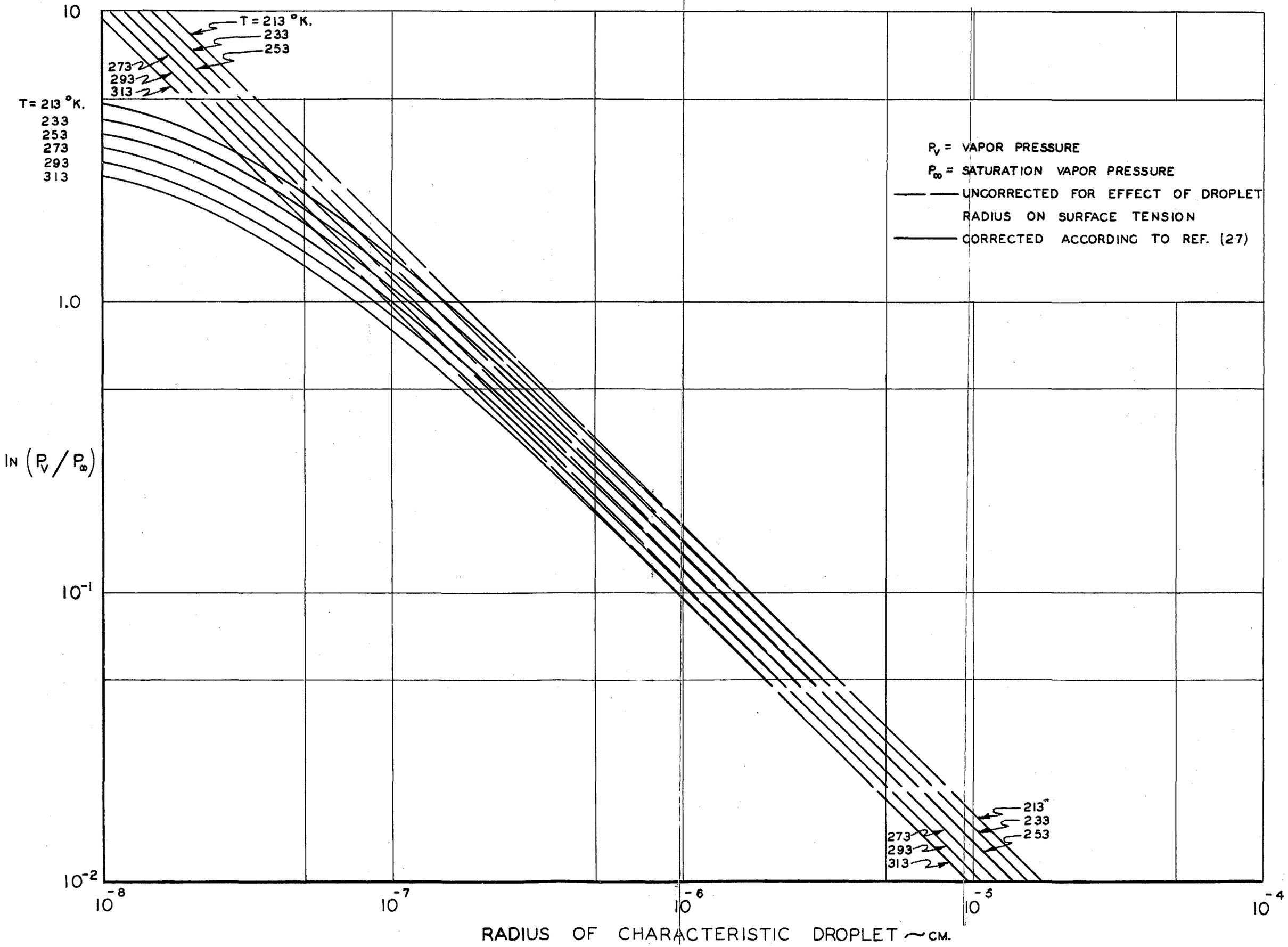

VARIATION OF RATE OF INCREASE OF SUPERSATURATION WITH TEMPERATURE

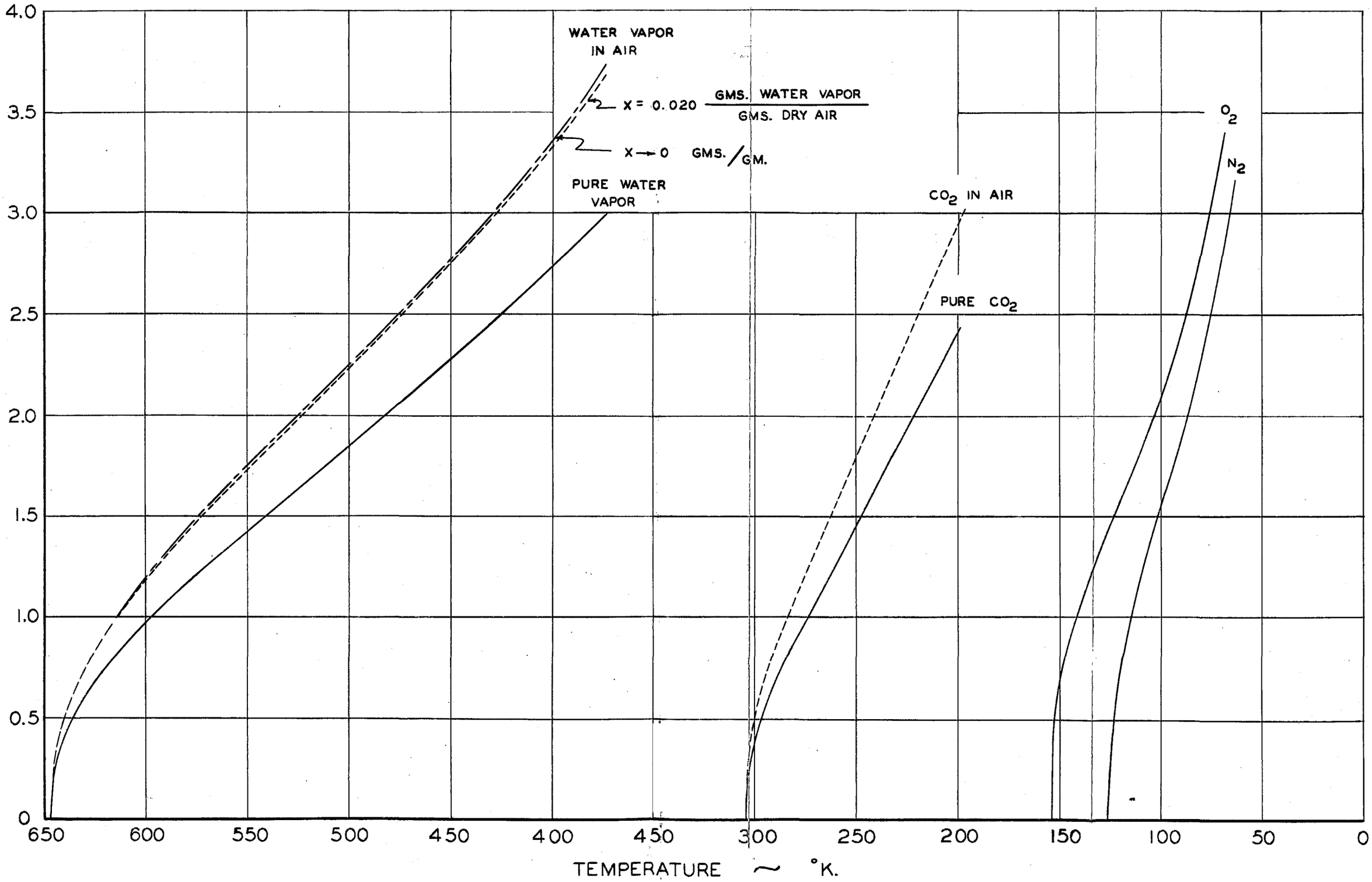

THRESHOLD SUPERSATURATION RATIO VS. TEMPERATURE

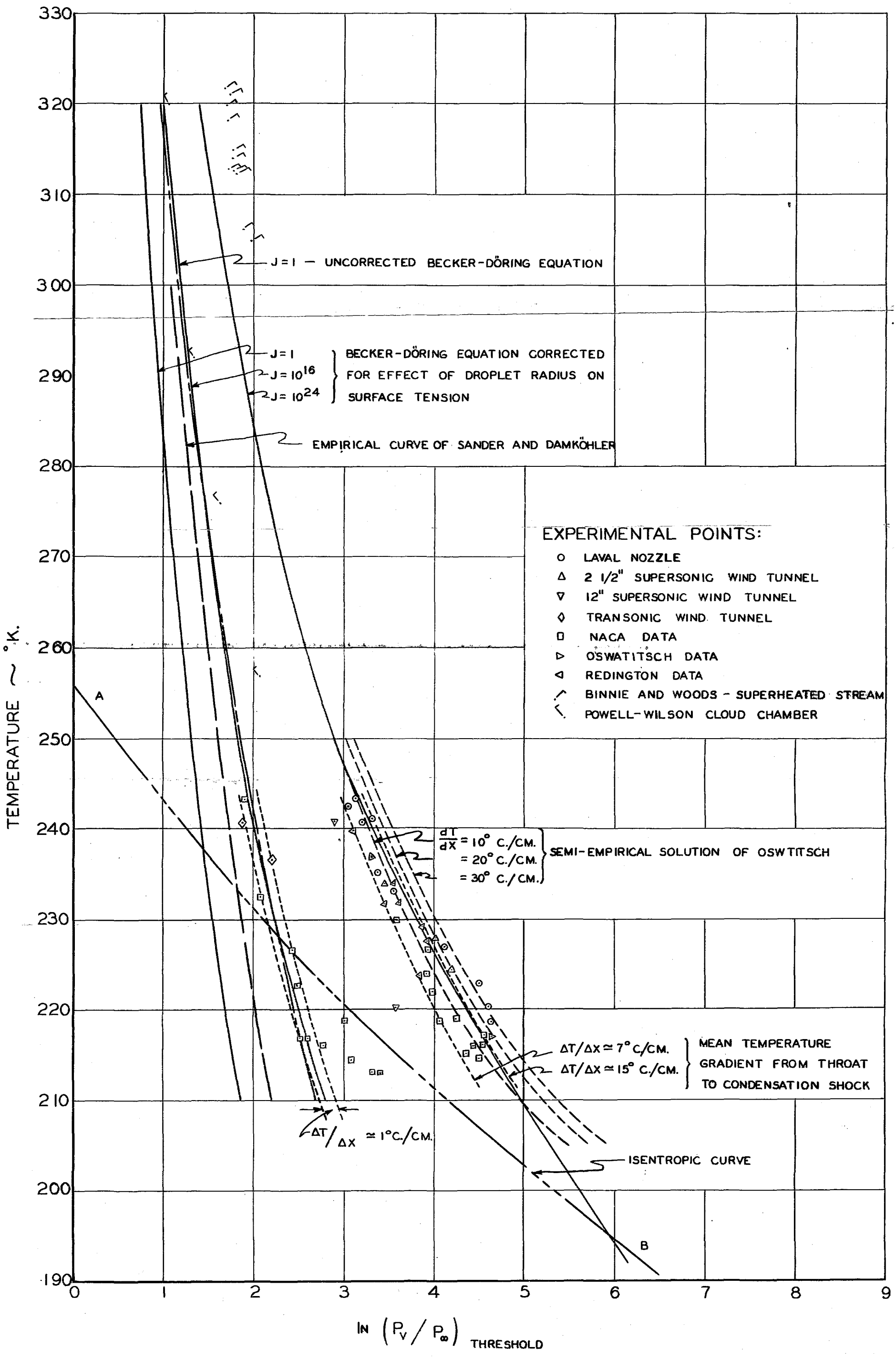

LAVAL NOZZLE
PRESSURE DISTRIBUTION MEASUREMENTS